Chapter 2

Chapter 2: Dendritic cell-targeted lentiviral vector immunization utilizes pseudotransduction and DNA-mediated STING activation

Published as: Jocelyn T. Kim, Yarong Liu, Rajan P. Kulkarni, Kevin K. Lee, Bingbing Dai, Geoffrey Lovely, Yang Ouyang, Pin Wang, Lili Yang, David Baltimore (2015). Dendritic cell-targeted lentiviral vector immunization utilizes pseudotransduction and DNA-mediated STING activation. *In review.*

ABSTRACT

Dendritic cell (DC)-targeted lentiviral vectors (LVs) deliver antigen and innate stimulation in vivo, resulting in strong T cell immunization. Here, we report that DC activation is triggered by cellular DNA packaged in LVs and is at least partially dependent on the STING protein. Activation is independent of MyD88, TRIF, and IPS-1, ruling out an involvement of Toll-like receptors or RIG-I-like receptor signaling. Further, we find that antigenic protein delivered in viral particles via pseudotransduction is sufficient to stimulate an antigen-specific immune response. Delivery of the viral genome encoding the antigen increases the magnitude of this response in vivo, but is irrelevant in vitro. Pseudotransduction, genomic transduction, and STING-mediated activation thus collaborate to make the DC-targeted LV a uniquely powerful immunogen.

INTRODUCTION

Dendritic cells (DCs) are critical to stimulating adaptive immune responses owing to their superior ability to process antigens and present them to T cells. Methods have been devised to directly target antigen to DCs for immunization purposes. One effective strategy uses an HIV-1-derived lentiviral vector (LV) to deliver genes encoding antigen to DCs as a T cell vaccine. LV can also target DCs by pseudotyping the vector with a mutant Sindbis virus glycoprotein (SVGmu), which binds to the DC-specific receptor DC-SIGN. The in vivo administration of this DC-targeted LV results in the selective expression of antigen in DCs and efficient priming of antigen-specific $CD8^+$ T cells with potent anti-tumor immunity in mice that out-performs conventional methods using recombinant protein antigen or adoptive transfer of antigen-loaded or viral vector-transduced DCs (Yang et al., 2008, Dai et al., 2009). Recent work has shown that this form of DC immunization is also effective in humans (Somaiah, 2015, Odegard et al., 2015). However, the exact mechanism behind such efficient immunization is not clear. It is evident that antigen delivery methods that lack a DC maturation signal — such as antigen conjugated to the DC-specific anti-DEC-205 antibody — lead to effective antigen presentation but promote tolerance rather than immunity (Bonifaz et al., 2002). The co-administration of anti-CD40 as a maturation stimulus is required to break immune tolerance. Thus, the success of DC-targeted LV immunization likely requires the coupling of two independent functions: delivery of antigen and activation of DCs.

The first function — antigen delivery to DCs — is thought to primarily occur by LV transduction (Cowan et al., 2002). However, transduction of differentiated DCs in vitro is notoriously difficult due to the host restriction factor SAMHD-1, which blocks reverse

transcription (Manel et al., 2010). The transduction of early stage or precursor DCs is more easily achieved, but these cells are not typically stimulated by the infection process (Dyall et al., 2001, He et al., 2005, Chinnasamy et al., 2000, Schroers et al., 2000, Breckpot et al., 2007, Rouas et al., 2002, Breckpot et al., 2003, Arce et al., 2009). Thus, it is not clear how LVs can concurrently deliver antigen and stimulate target DCs. One possibility is that another mechanism of protein antigen delivery exists besides transduction. For example, pseudotransduction is a process by which antigen expressed by the producer cells is carried by the vector into target cells (Haas et al., 2000, Nash and Lever, 2004, Breckpot et al., 2007). It is unknown if LV pseudotransduction plays a significant role in either antigen delivery and immune stimulation.

The second function — stimulation of DCs — is expected to occur through the triggering of host intracellular innate immune sensing pathways. Differentiated DCs are well activated by the LV transduction process (Yang et al., 2008, Dyall et al., 2001, Breckpot et al., 2010, Metharom et al., 2001, He et al., 2005). LV nucleic acids trigger endosomal Toll-like receptors (TLRs), which signal through the adaptor molecules MyD88 and/or TRIF (Breckpot et al., 2007, Beignon et al., 2005, Pichlmair et al., 2007, Breckpot et al., 2010). RNA helicase Rig-I-like receptors (RLRs), which signal through IPS-1 (also known as Cardif, MAVS, and VISA), detect cytosolic HIV genomic RNA (Berg et al., 2012). Finally, various cytosolic DNA sensors signal through the adaptor molecule STING (also known as TMEM173, MYPS, MITA and ERIS), and are involved in the detection of reverse transcribed lentiviral DNA (Jakobsen et al., 2013, Gao et al., 2013). However, it is not clear which of the LV components and intracellular innate immune

detection pathways is critical to DC activation and subsequent development of adaptive immunity.

Here we report LV pseudotransduction, a process by which antigen expressed by the producer cells is carried by the vector into target cells, contributes to antigen delivery, and is the primary mechanism of immune stimulation. LV transduction contributes to antigen delivery in vivo, but is not required for immune stimulation. In addition, LVs induced DC activation via the host STING pathway, independent of TLR and RLR signaling. We found encapsulated human genomic DNA is a previously unidentified constituent of virion preparations that can be recognized by the cytosolic DNA-sensing STING pathway.

RESULTS

LVs pseudotransduce DCs via protein delivery

We first sought to understand the mechanism of antigen delivery to differentiated DCs by LVs. We differentiated DCs by culturing mouse bone marrow cells and human monocytes in media containing the appropriate cytokines for eight days. We then treated these differentiated DCs with vesicular stomatitis virus glycoprotein (VSV-G)-pseudotyped LV expressing green fluorescent protein (GFP) at a multiplicity of infection (MOI) of one. The LV-treated DCs expressed a low but significant level of GFP by flow cytometry (**Figures S1A** and **S1C**), which was undiminished by reverse transcriptase inhibitors (RTIs) (**Figures 1A** and **1B**). By contrast, 293T cells treated with the same dose of LVs were efficiently transduced, as evidenced by a higher level of GFP expression, which was sensitive to RTIs (**Figures 1A** and **1B**). The expression of GFP

in DCs was highest immediately after LV treatment and then steadily decreased over 48 h (**Figure S1C**). In addition, we found that the protein synthesis inhibitor cycloheximide failed to decrease GFP expression, indicating that the GFP detected immediately after LV treatment was not produced de novo (**Figure 1C**). We also detected the protein GFP in LV lysate by Western blot analysis (**Figure 1D**), which indicated the presence of approximately one microgram of GFP per microgram of p24 by enzyme-linked immunosorbent assay (ELISA) (data not shown). This ability of LVs to incorporate vector-encoded protein was not specific to GFP because we also detected ovalbumin (OVA) in the lysate of LV encoding OVA (**Figure S2A**). These results are consistent with previous reports, indicating that LVs carry protein (Haas et al., 2000, Nash and Lever, 2004, Breckpot et al., 2007) and poorly transduce differentiated DCs in vitro (Schroers et al., 2000, Metharom et al., 2001, He et al., 2005, Manel et al., 2010). Retroviral particles have been found to carry cellular mRNA (Galla et al., 2004) and bacterial plasmids (Pichlmair et al., 2007), which could contribute to GFP expression in the target cell. However, since the GFP expression was insensitive to cycloheximide (**Figure 1C**), this suggests that GFP was not generated de novo in the DC, but likely delivered via pseudotransduction.

LV pseudotransduction of DCs induces activation

We next sought to determine whether LV pseudotransduction resulted in activation of differentiated DCs. We observed LV pseudotransduced mouse bone marrow derived DCs (BMDCs) were activated similarly to LPS treatment (**Figure S1B**). This activation was not diminished by RTIs, as demonstrated by the undiminished expression of DC activation markers CD86 and mouse MHCII molecule I-Ab (**Figure 1E**). LV

pseudotransduced human monocyte-derived DCs (moDCs) were also activated and unaffected by RTIs (**Figure 1F**). This lack of sensitivity to RTIs was not due to ineffective inhibition of reverse transcription because the RTIs significantly blocked GFP transduction in LV-infected 293T cells (**Figure 1A and 1B**). These results suggest that LV pseudotransduced DCs are activated by a reverse transcriptase-independent mechanism.

Viral envelope is an important immunostimulatory component

Next, we sought to systematically determine the LV component responsible for DC activation. We generated a platform of genome-less VLPs by exploiting the modularity of the LV system and omitted plasmids encoding the viral genome, capsid or envelope (**Figure 2A**) (Pichlmair et al., 2007, Mangeot et al., 2011). We confirmed the presence or absence of the viral envelope and capsid in these VLPs by Western blot analysis for VSV-G and p24 (**Figure 2B**). Similar to LVs, we found that pseudotyped VLPs incorporated vector-encoded proteins such as GFP or OVA (**Figures 2B** and **S2B**). However, "bald" viral particles, which were produced by transfecting 293T producer cells with the LV packaging plasmids encoding *gag*, *pol,* and *rev* (Cowan et al., 2002), were not capable of incorporating vector-encoded proteins. We next assessed whether these proteins were carried within the VLP or associated externally. We pre-treated VLP incorporating OVA with proteinase K, and then inactivated the proteinase K with phenylmethylsulfonyl fluoride (PMSF) before lysis of the particles, and still detected OVA in the VLP lysate, indicating that OVA was carried within the VLP (**Figure S2C**). If the proteinase K was not inactivated prior to particle lysis, OVA was no longer detected. We next determined whether VLPs were capable of delivering vector-encoded proteins to

DCs. We observed the VSV-G or SVGmu envelope was required for VLPs to deliver GFP into mouse BMDCs and human moDCs (**Figure 2C**). In addition, pseudotyped VLPs, but not "bald" VLPs, induced activation of DCs (**Figure 2D**). The inclusion of the vector genome or viral capsid had no effect on DC activation. Also, VLPs lacking the viral genome and capsid efficiently activated human moDCs (**Figure 2E**). Altogether these data suggest that the viral envelope, but not the vector genome or capsid, was necessary and sufficient to activate DCs.

LV genome, cDNA, and capsid are not required for immune stimulation in vivo

To determine whether these findings were relevant in vivo, we examined whether reverse transcription and the LV genome were required for LV immunization. Prior work demonstrated that LV expressing OVA and pseudotyped with SVGmu (LV-OVA) was DC-specific and elicited potent OVA-specific $CD8^+$ T cell responses (Yang et al., 2008). We injected the DC-targeted LV-OVA into mice with or without a concurrent oral regimen of RTIs. The administration of these RTIs was initiated one week prior to LV-OVA immunization and continued throughout the experiment. To determine the importance of the viral genome, we immunized mice with VLP carrying OVA pseudotyped with SVGmu (VLP-OVA). Both the LV-OVA and VLP-OVA used in this experiment carried OVA protein, the viral capsid, and the SVGmu envelope, but only the LV carried the viral genome. We pseudotyped all vectors used for immunization with the SVGmu envelope to limit off-target cell effects. We initially found OVA-specific effector memory $CD8^+$ T cells were similarly induced in mice treated with LV-OVA with or without RTIs or VLP-OVA at seven days post-immunization (**Figure 2F** top row). However, through ten days post-immunization, the magnitude of the OVA-specific $CD8^+$ T cells continued to

increase in LV-immunized mice, but not in the LV-OVA with RTIs or VLP-immunized mice (**Figure 2F** bottom row). After a second administration of homologous vector, the secondary OVA-specific $CD8^+$ T cell responses demonstrated more rapid kinetics and higher magnitudes than the primary immune response in all three groups (**Figure 2G**). In addition, these OVA-specific $CD8^+$ T cells expressed similar effector memory phenotypes ($CD62L^{lo}CD44^{hi}$) in all three groups (**Figure 2H**). The primary and secondary immunization responses were similar between the mice receiving LV with RTIs and VLP, suggesting that a component of LV immunization is independent of reverse transcription and the viral genome, thus, likely due to pseudotransduction.

After the secondary immune responses subsided, we next assessed the in vivo function of the prime-boosted $CD8^+$ T cell responses using an OVA-expressing tumor model. We injected OVA-expressing tumor cells and control non-OVA-expressing tumor cells on opposing legs, enabling intra-animal comparison. Mice homologously primed and boosted with LV with or without RTIs or VLPs were effectively protected against the growth of OVA-expressing tumors (**Figure 2I**). The non-OVA-expressing tumor cells continued to grow in the mice as expected. The efficient anti-tumor protection of LV with RTI and VLP-immunized mice is not altogether surprising since 8-10% of the $CD8^+$ T cells were OVA-specific after the boost. Therefore, the vector genome and its transduction enhanced, but were not necessary to inducing memory $CD8^+$ T cells. These results suggest that LV pseudotransduction is sufficient to induce a functional memory $CD8^+$ T cell response.

To investigate the immunostimulatory effect of the viral capsid and envelope we homologously prime-boosted mice with VLPs carrying OVA with or without the viral capsid (VLP-OVA or VLP-OVAΔgag, respectively). Both immunization groups developed similar primary and secondary $CD8^+$ T cell responses and were effectively protected against the growth of OVA-expressing tumors (**Figures 2J** and **2K**). Therefore, VLPs, which have the viral envelope as the sole viral component, generated a sufficiently strong memory $CD8^+$ T cell response protective against the growth of OVA-expressing tumor cells. The viral capsid did not enhance immunization responses. Thus, the viral envelope of the vector is sufficient in stimulating LV immunization responses in vivo.

LV transduction enhances antigen delivery

We next aimed to understand why LV immunization generated a higher magnitude of memory $CD8^+$ T cells compared to LV with RTI or VLP immunizations. We hypothesized that LV transduction contributes to antigen delivery rather than immune stimulation. We generated an SVGmu-pseudotyped LV encoding GFP and carrying the protein OVA (LV-GFP^{gene}-$OVA^{protein}$) by transiently transfection of 293T cells with the plasmids required to produce GFP-expressing LV and an expression plasmid for OVA. Because the vector in these virions did not encode OVA, the OVA-specific $CD8^+$ T cells induced would be a result of LV pseudotransduction. Additionally, because this vector was capable of reverse transcription, it would indicate if reverse transcribed LV DNA was an immune adjuvant. This vector induced an OVA-specific $CD8^+$ T cell response similar to VLP-immunized mice (**Figure 2L**), suggesting that reverse transcribed LV DNA itself is not an immune adjuvant to the antigen-specific $CD8^+$ T cell response produced by

pseudovirions. There should not be antigenic competition between GFP and OVA because GFP is minimally antigenic and fails to elicit a GFP-specific $CD8^+$ T response in C57/B6 mice (Skelton et al., 2001). Thus, this data suggests antigen delivery during LV immunization is an additive process between pseudotransduction and transduction. However, LV genome transduction does not appear to contribute to immune stimulation.

LVs activate DCs and adaptive immunity via STING pathway

We next set out to identify the innate immune signaling pathway responsible for LV detection, DC maturation, and subsequent priming of $CD8^+$ T cells. We treated BMDCs from mice deficient in MyD88, TRIF, or IPS-1 with an LV expressing GFP pseudotyped with VSV-G or SVGmu. Consistent with prior work, we found that the two vectors, VSV-G and SVGmu-pseudotyped LVs, similarly activated wild-type BMDCs (**Figure S1**). We observed that LVs capably activated BMDCs from mice deficient in MyD88, TRIF, or IPS-1 (**Figure 3A**). To examine the possibility of redundant pathways, we treated BMDCs from mice doubly deficient in MyD88 and TRIF or MyD88 and IPS-1 with LV and found that DC activation was still unaffected (**Figures S3A** and **S3B**). To study activation of DCs in vivo we injected the DC-targeted LV-OVA into mice deficient in MyD88, TRIF, or IPS-1 and measured OVA-specific $CD8^+$ T cells. We found that OVA-specific effector memory $CD8^+$ T cells fully developed in mice deficient in MyD88, TRIF, or IPS-1 at similar levels to wild-type mice (**Figures 3B**-**3E**). These findings suggest that LV innate immune detection and subsequent adaptive immunity do not depend on TLR and RLR signaling pathways.

We turned to the STING-signaling pathway, an important adaptor protein involved in cytosolic viral DNA sensing. To address whether STING was important in LV detection, we injected STING-deficient mice with the DC-targeted LV-OVA and found a significantly diminished OVA-specific $CD8^+$ T cell response compared to wild-type mice immunized with LV-OVA (**Figures 3E** and **3F)**. Consistent with other work, we noted normal T cell subsets in unimmunized STING-deficient mice (**Figure S4**) (Ishikawa et al., 2009). These results indicate that LV activation of DCs and $CD8^+$ T cell response is partially dependent on STING.

VLPs activate DCs and adaptive immunity via STING pathway

We next investigated whether the reverse transcribed LV DNA was required to induce the STING-dependent immune response. We infected mouse BMDCs from STING-deficient mice with VSV-G or SVGmu-pseudotyped VLP carrying GFP and found that maturation was partially dependent on STING (**Figure 4A**), suggesting a component other than the viral genome could activate STING. In addition, STING-deficient BMDCs treated with VLP carrying OVA had a reduced ability to activate OT-1 $CD8^+$ T cells, which express an OVA-specific TCR, as demonstrated by the reduced expression of T cell activation surface markers, CD69 and CD25 (**Figure 4B**). We next treated STING-deficient mice with a homologous prime-boost vaccination of the DC-targeted VLP-OVA, which lacked the LV genome and capsid, and observed significantly less effector memory $CD8^+$ T cells in the STING-deficient mice (**Figures 4C-4E**). Altogether, these results demonstrate that a component other than the lentiviral genome or reverse transcribed LV DNA can trigger the host STING pathway.

Viral fusion is required for DC activation

Since we found that the viral envelope was necessary and sufficient for stimulating DCs, we next focused on understanding this mechanism of activation. The viral envelopes of vesicular stomatitis virus and Sindbis virus induce cell-surface receptor mediated endocytosis and release viral contents into the cytosol through pH-dependent viral fusion between the viral envelope and host endosomal membrane (Florkiewicz and Rose, 1984, Smit et al., 1999). To investigate the importance of viral fusion on DC activation, we treated mouse BMDCs with pseudotyped VLPs devoid of the LV genome and capsid or LVs in the presence of the fusion inhibitor chloroquine (Dille and Johnson, 1982). We observed that DC activation by VLPs and LVs was abolished in the presence of chloroquine (**Figure 5A**). This effect was not due to lack of internalization because intracellular punctate GFP was evident in the chloroquine-treated cells (**Figure 5B**). We next used an altered VSV-G, in which mutations rendered the protein fusion-defective without altering envelope binding or receptor-mediated endocytosis (Zhang and Ghosh, 1994). BMDCs treated with fusion-competent VLP displayed diffuse intracellular GFP presence by microscopy, whereas DCs treated with the fusion-defective VLP showed punctate GFP presence similar to chloroquine-treated cells (**Figure 5B**). We also observed the fusion-defective LV and VLP failed to activate mouse BMDCs (**Figure 5C**). Thus, these findings suggest that viral fusion is required for LV and VLP activation of DCs.

We next asked whether the viral process of membrane fusion itself and/or the release of a putative activating component into the cytosol represented the activating stimuli. To first determine whether VSV-G-mediated fusion itself was immunostimulatory we

incorporated VSV-G into the lipid membrane of non-cationic multilamellar liposomes, which allows for the liposomal contents to evade lysosomal degradation and be delivered into the cytosol via viral envelope-directed fusion (Abe et al., 1998). Indeed, we observed that delivery of GFP into mouse BMDCs by GFP-carrying liposomes was greatly enhanced if the liposomes were enveloped with VSV-G (**Figure 5D**). Additionally, maturation of DCs was increased if liposomes were enveloped with VSV-G, suggesting that VSV-G-directed fusion was immunostimulatory. To determine whether VSV-G-directed fusion induced DC activation via STING, we treated STING-deficient mouse BMDCs with VSV-G liposomes and found that DC maturation was unaffected (**Figure 5E**). These results suggest that VSV-G-directed fusion itself induces DC activation in a STING-independent manner. Thus, there appears to be two separate activating processes at work when enveloped particles stimulate DCs: one is STING-dependent and the other is STING-independent. These findings suggest the STING-independent process is activated by envelope protein-directed fusion. What then activates the STING-dependent process? It seemed likely that a stimulatory viral component was released into the cytoplasm by viral fusion.

Lentiviral particles and VLPs contain human DNA

We next attempted to identify an immunostimulatory component that might be released by LVs or VLPs. Since STING is involved in cytosolic dsDNA recognition, we suspected that LVs and VLPs might contain non-viral DNA. Indeed, plasmid DNA used during LV production has been detected inside LV particles (Pichlmair et al., 2007). Consistent with this work, we amplified plasmid-specific DNA sequences of the VSV-G and ampicillin resistance genes in the LV and VLP preparations by PCR. Interestingly, we

also amplified DNA sequences for human beta-actin and human Alu repeat element in LV and VLP preparations (**Figures 6A, S5A, and S5B**). We did not find evidence of human DNA in cell-free supernatant collected from 293T cells transfected with a mock plasmid (**Figures 6A and S5B**). To assess whether the plasmid and human DNA were carried within or associated externally to the particles, we pre-treated VLPs with DNase I to degrade external DNA, and then inactivated DNase I with EDTA before particles were lysed and then analyzed by PCR. Despite pre-treatment with DNase I, we continued to detect plasmid and human DNA in the vector preparations, suggesting plasmid and human DNA was contained within the particles (**Figure 6B**). We used genomic DNA to show DNase I digestion was efficient and DNase I inactivation with EDTA was effective (**Figure 6C**). We also amplified plasmid and human DNA in the cell-free supernatant of 293T cells transfected with a plasmid encoding HIV-1 (**Figure 6D**). Therefore, these results suggest that LV, VLP, and infectious HIV-1 particles, which are produced by transient transfection of 293T cells, contain both plasmid and human genomic DNA.

To determine whether the presence of DNA in particles was particular to material made in 293T cells, we asked whether HIV-1 passaged in human PBMCs also contained human genomic DNA. Interestingly, we were able to amplify human DNA from the cell-free HIV-1 supernatant collected after passage the virus in human PBMCs (**Figures 6E**). Human DNA was not detected in the cell-free supernatant collected from uninfected PBMCs. In addition, we found that the DNA detected in the passaged cell-free HIV-1 supernatant was resistant to DNase I (**Figure 6F**), suggesting that human genomic DNA was also encapsulated inside HIV-1 particles.

Human DNA delivered into DCs by VSV-G fusion is immunostimulatory

We next questioned whether the delivery of plasmid or genomic DNA by viral fusion would enhance the DC activation generated by viral fusion itself. Therefore, we exposed mouse BMDCs to empty VSV-G liposomes or VSV-G liposomes carrying plasmid DNA or genomic DNA extracted from 293T cells. As expected, we found VSV-G liposomes induced DC maturation (**Figure 6G**). The addition of human genomic DNA into VSV-G liposomes resulted in even higher levels of DC activation. We then found that the enhancement in DC activation due to human DNA was abrogated in STING-deficient BMDCs (**Figure 6H**). These results suggest that both viral fusion itself and viral-fusion-dependent delivery of human DNA are able to induce DC maturation, the former in a STING-independent and the latter in a STING-dependent manner. These findings provide an explanation for the STING-dependence observed in the innate and adaptive immune responses generated by LVs and VLPs.

DISCUSSION

From our previous work we knew that DC-targeted LVs deliver antigen to DCs and stimulate a massive antigen-specific $CD8^+$ T cell response in vivo (Yang et al., 2008), which was consistent with previous work demonstrating LVs activate innate and adaptive immunity (Granelli-Piperno et al., 2000, He et al., 2005, Dullaers et al., 2006, Esslinger et al., 2003). In the present investigation, we examined why LVs are so effective at these processes. We were especially interested in understanding how these vectors deliver antigen and provide immune stimulation. We found that there were four components of the virions contributing to the immunization process.

First, we found that vector-encoded protein antigen is carried over from the producer cells in the vector particles via pseudotransduction. Previous reports of pseudotransduction (Haas et al., 2000, Nash and Lever, 2004, Breckpot et al., 2007) have not appreciated how effectively this process delivers antigen to differentiated DCs. We observed that the in vivo administrations of DC-targeted LV in the presence of RTIs and VLP immunization were sufficient in producing antigen-specific $CD8^+$ T cells, suggesting LV pseudotransduction alone capably delivers antigen and simulates the immune system.

Second, we found that the delivery of the LV genome was important to antigen expression, but not immune stimulation. Mice immunized with a LV encoding GFP and carrying the protein OVA (LV-GFP^{gene}-$OVA^{protein}$) had similar immune responses to VLP-OVA immunized mice. These results strongly imply that the viral genome of the LVs, in the form of reverse transcribed DNA, encodes antigen and contributes to antigen delivery, but not to immune stimulation. This is consistent with our in vitro results showing virtually all of the antigenic stimulation of differentiated DCs is due to pseudotransduction because activation is not sensitive to RTIs and efficiently occurs with viral genome-deficient vectors. The cells transduced by our DC-targeting LV in vivo may be early stage DCs, which are relatively easier to transduce, but resistant to stimulation compared to differentiated DCs (Chinnasamy et al., 2000, Rouas et al., 2002, He et al., 2005, Schroers et al., 2000). The mechanism of how transduced cells contribute to antigen delivery has yet to be defined. Since our data and previous work suggest that LV transduction is not stimulatory, it is possible that antigen in transduced

cells may be indirectly presented or cross-presented to the immune system (He and Falo, 2007). Altogether, our results further clarify the role of true LV infection in vivo.

Third, we found that the activation of DCs (assayed by the appearance of activation marker proteins on the cell surface) was partly a consequence of fusion between the LV membrane and the endosomal membrane. We showed that particles must be internalized (bald particles were ineffective) and then fused with endosomal membranes (active viral fusogen is needed and chloroquine, which inhibits endosome acidification, or fusion-defective vectors abolish DC activation). This process did not require STING, an endoplasmic reticulum-resident protein and adaptor protein for cytosolic DNA detection pathways.

Fourth, we investigated what other mechanisms might be involved in DC activation. By using various knockouts, we found that neither a TLR nor RIG-I was involved. Rather, DC activation was partially dependent on STING. Our study identified cellular DNA packaged from producer cells as the component of the virion that is sensed by STING. This is consistent with previous reports showing cytosolic dsDNA is a well-known activator of innate immunity through STING (and cyclic GMP-AMP synthase (cGAS)) (Gao et al., 2013, Jakobsen et al., 2013). Thus, the fourth component of the virion that contributes to LV immunization is encapsulated human DNA. Current work is underway to examine the role of cGAS, which recognizes cytosolic dsDNA and signals upstream of STING (Sun et al., 2013).

Our study sheds new light the mechanism of DC vaccination by LVs. We have found that antigen delivery is an additive process between LV pseudotransduction and transduction. However, LV immune stimulation is induced primarily by LV pseudotransduction. We had expected that TLR or RIG-I activation of innate immune responses was important based on previous work suggesting the importance of MyD88 and TRIF in DC activation in vitro and in vivo (Breckpot et al., 2007, Pichlmair et al., 2007). However, we found that neither TLR nor RIG-I signaling was involved. Rather, activation was partially dependent on STING. The differing results of our study may be because we injected a DC-targeted LV into mice to determine the direct effects of LVs on DCs in vivo. Previous work used adoptive transfer experiments to infer the in vivo effect of LVs on DC activation (Breckpot et al., 2007, Pichlmair et al., 2007). In addition, we found viral fusion itself and viral-fusion-dependent delivery of human DNA induced DC maturation, the former in a STING-independent and the latter in a STING-dependent manner. One group has also observed that STING was required to generate type I interferon responses to the fusion (Holm et al., 2012) by herpes VLPs and cationic liposomes. Herpes VLPs have different mechanisms of entry compared to our VSV-G and SVGmu-pseudotyped VLPs. Additionally, the mechanism of entry of cationic liposomes is not fully elucidated is not fully elucidated and does not follow classical fusion utilized by enveloped viruses (Elouahabi and Ruysschaert, 2005). Thus, we used VSV-G enveloped liposomes to study viral fusion itself.

Our findings raise important questions regarding the nature of particles in virus preparations. Previous work has suggested that HIV particles passaged in T cells are a mixture of replication-competent and replication-defective particles, the latter being more

abundant (Bernier and Tremblay, 1995). In addition, the expression of glycoproteins of vesicular stomatitis virus and Sindbis virus in 293T producer cells results in the spontaneous shedding of enveloped particles (Moore et al., 2006, Mangeot et al., 2011). Thus, we suspect that virus preparations contain a mixture of particles with and without the viral RNA genome. We are uncertain whether only one or both types of particles contain the protein and cellular DNA that are involved in DC stimulation and T cell response. Separation of the various types of particles has been difficult, but with the improvement and accessibility of single nanoparticle sorting, the answers to these questions are now within our reach.

In addition, we assume that the vector-encoded protein contained in the viral particles is merely encapsulated cytoplasm because we found both OVA and GFP in the particles. However, there may be more specific interactions involved. How DNA is packaged within particles is more of a mystery. HIV infection induces cell death by pyroptosis, a process that leads to DNA fragmentation (Doitsh et al., 2014). It could be that as cells die, the HIV particles being produced pick up fragmented DNA from the host cell. We also detected human genomic DNA within LV and VLP particles, the formation of which should not involve pyroptosis. The ability of LVs and VLPs to package human genomic DNA may be a result of liposomal transfection reagents, which are cyto- and genotoxic, inducing host DNA damage and increasing cytosolic dsDNA in cells (Knudsen et al., 2015, Shen, 2014). Thus, the fragmented, cytoplasmic genomic DNA may be available for encapsulation in many cell types via different processes. Further studies are needed to determine the immunologic significance of human genomic DNA delivered by viral particles.

This study began as an investigation of a particular form of technology, DC-targeted LV. As the work has progressed, aspects of viral interaction with host immunity have become evident and that have helped to understand the transduction process but have raised multiple questions about what is delivered by viral vectors. Our findings suggest that cellular DNA may act as a viral ligand to the STING pathway. The development of DNA adjuvants that serve as STING agonists could provide a new therapeutic strategy for inducing $CD8^+$ T cell responses. Additionally, our finding that lentiviral vectors package tumor cell DNA from producer cells raises a potential safety concern for viral vector-based gene therapies, which merit further investigation.

EXPERIMENTAL PROCEDURES

Statistics, sample size selection, and exclusion criteria. All experimental group sizes were selected to ensure adequate statistical power despite the variable nature of the studies performed. No animals were excluded from the study. Groups of animals were chosen in consecutive order and were not randomized prior to commencing the study. Animal studies were not performed in a blinded fashion.

Mice. C57BL/6J, MyD88$^{-/-}$, TRIF mutant (C57BL/6J-Ticam1^{Lps2}), Tmem173$^{-/-}$, and OT-I (C57BL/6-Tg(TcraTcrb)1100Mjb/J) mice were obtained from The Jackson Laboratory. IPS-1$^{-/-}$ mice were provided by G. Cheng (UCLA). MyD88$^{-/-}$/Ticam1$^{Lps2/Lps2}$ and MyD88$^{-/-}$ /IPS-1$^{-/-}$ mice were generated and bred. p50$^{-/-}$ mice have been described (Sha et al., 1995). All mice were maintained on the C57BL/6J background and used according to protocols approved by Institutional Animal Care and Use Committee at Caltech. Experiments were performed with mice 6-12 weeks of age with sex-matched littermates.

Antibodies and flow cytometry. Single-cell suspensions were stained with the following antibodies from Biolegend: Pacific blue-anti-mouse CD11b (117321), pacific blue-anti-mouse CD44 (103020), PE-anti-mouse CD62L (104408), PE-anti-human CD11c (301606), PE/Cy7-conjugated anti-mouse I-Ab (115420), PE/Cy7-anti-mouse CD69 (104512), PerCP-anti-human CD14 (325621), APC-anti-mouse CD11c (11730), APC-anti-human CD86 (305411), APC/Cy7- anti-mouse CD86 (105030), and APC/Cy7-anti-human HLA-DR (307617). For dead cell staining, 1ug ml^{-1} of propidium iodine was added. APC-conjugated H-2K^{b} tetramers bound to the OVA-derived peptide SIINFEKL

were obtained from the NIAID Tetramer Facility. Cells were analyzed on a MACSQuant analyzer (Miltenyi), data were analyzed with FlowJo software (TreeStar).

Isolation and culture of DCs. Differentiation of mouse BMDCs was achieved by culture for 8 d in media containing granulocyte-macrophage colony-stimulating factor (GM-CSF) (1:25 J558L conditioned medium) as previously described (Dai et al., 2009). Human moDCs were generated by culture for 8 d of $CD14^+$ peripheral blood monocytes (UCLA Center for AIDS Research (CFAR) Virology Core Lab) in media containing human GM-CSF and IL-4 (Peprotech). BMDCs and moDCs were cultured in RPMI-1640 medium supplemented with 10% (vol/vol) fetal bovine serum (FBS) (Sigma), 1% (vol/vol) non-essential amino acids (HyClone), 1mM sodium pyruvate (Gibco), 10mM HEPES (Gibco), and 0.05mM 2-mercaptoethanol (Gibco).

Cell lines. HEK293T/17 cells (ATCC) and 293T.DCSIGN cells, which were generated as previously described (Yang et al., 2008), were cultured in DMEM with 10% (vol/vol) FBS. EL4 (C57BL/6J, $H\text{-}2^b$, thymoma) and E.G7 (EL4 cells stably expressing one copy of chicken OVA cDNA) provided by L. Yang (UCLA) and GXR.CEM human lymphoblastoid $CD4^+$ T cells provided by B. Walker (Ragon Institute) were cultured in RPMI-1640 medium with 10% (vol/vol) FBS. All media was supplemented with 1% (vol/vol) penicillin and streptomycin (Gibco).

LV, VLP, and infectious HIV-1. The LV transfer vectors (FUGW, FOVA) used in this study are the third generation HIV-based LVs. FUGW encodes the GFP and FOVA encodes an invariant chain-OVA fusion construct as previously described (Hu et al.,

2011). The plasmids pMDLg/pRRE encoded *gag* and *pol* and pRSV-Rev encoded *rev*. The envelope plasmids used were p.VSV-G and p.SVGmu (Yang et al., 2008). Introducing mutations G124A and P127A as previously described (Zhang and Ghosh, 1994) generated the fusion-defective VSV-G. The pNL4-3 plasmid used to generate infectious HIV-1 was obtained from the AIDS Reagent Program, Division of AIDS, NIAID, NIH. Virus was prepared by culturing HEK293T/17 cells in 10-cm tissue culture dishes and transfecting with BioT (Bioland Scientific, Paramount CA) according to manufacturer's instructions using a total of 10 μg DNA. For production of LV, we used the LV transfer vector plasmid, which encodes the viral genome (4 μg), and 2 μg each of the packaging plasmids (pMDLg/pRRE, pRSV-Rev), and the envelope plasmid (VSVG, SVGmu, VSVG.fd). LV encoding GFP used the LV transfer vector plasmid FUGW and LV encoding OVA used the LV transfer vector plasmid FOVA. To generate LV encoding GFP and carrying OVA, the plasmids FUGW, pMDLg/pRRE, pRSV-Rev, p.SVGmu, and an expression plasmid encoding the invariant chain-OVA fusion construct (p.OVA) were used. To generate VLPs lacking a viral genome, the LV transfer vector plasmid was omitted. Capsid deficient vectors were generated by omitting the packaging plasmids pMDLg/pRRE and pRSV-Rev. Consistent with previous findings, transfection of 293T producer cells with the LV packaging plasmids encoding *gag*, *pol* and *rev* generated “bald” particles (Cowan et al., 2002). To generate VLPs carrying GFP or OVA, an expression plasmid encoding GFP (p.GFP) or p.OVA was included during transfections. Puc19 plasmid was transfected into 293T cells as a negative control. To generate an infectious molecular clone of HIV-1, 20 μg of pNL4-3 plasmid was used for transfections. All viral supernatants were harvested at 36, 48, and 60 h post-transfection and filtered through a 0.45-μm filter. The cell-free LV and VLP supernatants were additionally

ultracentrifugated (Optima L-80 K preparative ultracentrifuge, Beckman Coulter) at 80,000 *g* for 90 min through a 20% (vol/vol) sucrose cushion. The pellets were then resuspended in an appropriate volume of cold PBS. 293T and 293T.DCSIGN cells were infected with LV and cells analyzed for GFP expression by flow cytometry to determine the transduction titer by the dilution ranges that exhibited a linear response. The concentration of gag was measured by p24 capture ELISA Kit (ImmunoDiagnostics) and GFP by GFP ELISA Kit (Abcam). The concentration of iOVA was determined using a sandwich ELISA. The 96-well plates were coated with anti-CD74 at 5 μg ml^{-1} (555317; BD Biosciences) and blocked with PBS containing 1% (vol/vol) BSA. The vectors were lysed in 0.5% (vol/vol) Triton X-100 and incubated on coated plates. The amount of captured OVA was determined using anti-chicken OVA at 5 μg ml^{-1} (1221; Abcam). Detection was performed using a horseradish peroxidase-conjugated goat-anti-mouse IgG (Bethyl Lab) at a dilution of 1:10,000. Colorimetric analysis was performed using TMB Peroxidase Substrate System (KPL) and absorbance was read at 450nm.

DC treatment with vectors. DCs (1–2 × 10^6 cells) were centrifuged with LV (1–2 × 10^6 transduction units; 100–200 ng of p24, GFP, or OVA) or VLP (100–200 ng of p24; 100–200 ng of GFP) at 1,050 *g* at 30 °C for 90 min. After centrifugation, the supernatant was removed and replaced with fresh medium and cytokines and incubated at 37 °C with 5% of CO_2. Post-treatment, the supernatant was removed and replaced with fresh medium containing cytokines and incubated at 37 °C with 5% of CO_2. Cycloheximide (CHX) and chloroquine (CQ) (Sigma) were added to cell cultures 1 h prior to LV treatment and was added back to the fresh medium. Tenofovir (TFV) and efavirenz (EFV) (AIDS Research

and Reference Reagent Program, NIAID/NIH) were added to cell cultures 6 h prior to LV treatment and after centrifugation drugs were added to the fresh media.

Mouse immunization and tumor challenge. LVs and VLPs were injected subcutaneously into the right flank of mice. Priming immunization contained between 25-–50 ng of p24. All vectors were normalized to equivalent amounts of OVA and/or p24 by ELISA. During prime-boost immunization, the vector doses of the prime and boosts were identical. Blood was collected from the immunized mice and PBMCs processed and analyzed for the presence of OVA-specific T cells using a Class I H-2K^{b}-SIINFEKL tetramer and their surface activation markers using flow cytometry. For homologous boosts, mice received the same dose of LV and VLP in the right flank. Unimmunized mice received equal volume injections of PBS. For the tumor protection experiments, mice received 1–5×10^{6} EL4 or E.G7 cells injected subcutaneously into the opposing flanks of the mice. Tumor size was measured and shown as a product of the two largest perpendicular diameters $a \times b$ (mm^{2}). In these experiments, the mice were killed when the tumors reached 200 mm^{2}. In the experiments using reverse transcriptase inhibitors (RTIs) in vivo, tablets containing efavirenz 600 mg, emtricitabine 200 mg, and tenofovir disoproxil fumarate 300 mg were crushed, resuspended in PBS containing 1% (vol/vol) DMSO, filtered through a 0.22 μm filter, and stored in aliquots at –80 °C. RTIs were added to the fresh drinking water of mice at the following approximate concentrations: efavirenz 10mg ml^{-1}, emtricitabine 3.6 mg ml^{-1}, tenofovir 5.4mg ml^{-1}. Fresh water containing RTIs was replaced two times a week. Mice receiving no RTIs were given similar volumes of drinking water and replaced accordingly. Mice were initiated on the

oral regimen of RTIs one week prior to immunization and continued throughout the duration of the experiment.

Immunoblot analysis. Vector preparations were lysed in 1% Triton X-100 in PBS supplemented with HALT protease and phosphatase inhibitor cocktail (Life Technologies) and clarified by centrifugation. Aliquots of the lysate were mixed with non-reduced Laemmli's sample buffer and resolved by 5–15% (wt/vol) SDS-PAGE. After transfer to nitrocellulose, the following antibodies were used: GFP (8334; Santa Cruz), OVA (1221; Abcam), VSVG (v5507; Sigma), and p24 (10R-H120b; Fitzgerald). To determine if proteins were inside the vector particles, samples were pre-treated with proteinase K 10 μg ml^{-1} (Qiagen) and incubated at 55 °C for 1 h, and then the proteinase K was inactivated with PMSF 1mM (Sigma) before samples were lysed.

In vitro DC stimulation of OT-1 cells. Mouse BMDCs were spin-infected with VLPs carrying OVA, and washed and resuspended in fresh media and 1 μg ml^{-1} LPS). $CD8^+$ T cells were purified using MACS Columns (Miltenyi) from the spleen cells of OT-1 transgenic mice and cultured with the uninfected or VLP-infected BMDCs at a ratio of 1:1. The cells were collected and analyzed for their surface activation markers using flow cytometry 24 h after co-culture. Splenocytes were collected from STING-deficient and wild-type mice and treated with PMA (50 ng ml^{-1}) and Ionomycin (500 ng ml^{-1}) for 24h, 48h, and 72 h. Cells were then collected and analyzed for their surface activation markers using flow cytometry.

Fluorescent imaging. Cells were washed once with cold PBS and then fixed using 4% (vol/vol) cold paraformaldehyde in PBS (10 min at 22 °C) followed by washing 4 times with cold PBS. Images were collected using a fluorescence microscope (Axiovert 200m; Zeiss) equipped with three filter wheels (Lambda 10-3; Sutter Instruments), and a cooled CCD camera (Evolution/Qimaging; Media Cybernetics). Images were collected using Image-ProPlus 5.1 software (Media Cybernetics). All data within each experiment were collected at identical imaging settings; relevant sets of images were adjusted only for brightness/contrast.

Liposomes. Multilamellar liposomes were prepared based on the conventional dehydration-rehydration method as previously described (Liu et al., 2014). DOPC, DOPG and MPB-PE (NOF Corporation) were combined in chloroform, at a molar lipid ratio of DOPC:DOPG:MPB = 4:1:5, and the organic solvent in the lipid mixture was evaporated under argon gas. The lipid mixture was further dried under vacuum overnight to form dried thin lipid films. The resultant dried film containing 1.12 ug of lipids was hydrated in 10 mM Bis-Tris propane at pH 7.0 with GFP (STA-201; Cell Biolabs) at a concentration of 125 ng ml^{-1} in a total volume of 300ul. Polyhistidine tagged VSV-G was expressed and purified from a suspension 293-E cells after a 48-h transfection using Ni-NTA column purification. Purified VSV-G protein (200 µg ml^{-1}) was added to the lipid hydration mixture before sonication. Alternatively, 5 ml of VSV-G enveloped VLPs, collected from the medium of 293T cell transfected with p.VSVG and purified and concentrated as described above, was added to the lipid hydration mixture, as previously described (Abe et al., 1998), and DNA was not detectable by PCR in the liposomes made by this method. To add DNA into the liposomes, 30 µg ml^{-1} of genomic

DNA extracted from 293T cells or plasmid DNA was added to the lipid hydration mixture. Lipid film and hydration mixture were vigorously vortexed every 10 min for 1 h, and then applied with 4 cycles of 15 s sonication (Misonix Microson XL2000) on ice in 1 min intervals for each cycle. To induce divalent-triggered vesicle fusion, $MgCl_2$ was added at a final concentration of 10 mM. The resulting multilamellar vesicles were further cross-linked by addition of Dithiothreitol (Sigma) at a final concentration of 1.5 mM for 1 h at 37 °C. The resulting vesicles were collected by centrifugation at 14,000 *g* for 4 min and then washed twice with PBS.

DNA analysis. Virus and VLP samples were inactivated/lysed by heating to 95 °C for 15 min. To determine whether DNA was carried within the particles, virus and VLP samples were pre-treated with DNase I (Sigma) at a final concentration of 0.1 mg ml^{-1} at room temperature for 10 min, and then the DNase I was inactivated with EDTA 0.625 mM at 70 °C for 10 min, before inactivation/lysis. To show that DNase I degradation was complete, DNase I was not inactivated by EDTA prior to lysis. PCR amplifications from samples were carried out in 0.2-mL thin-walled reaction vessels in the Eppendorf Mastercycler proS. The manufacturer-supplied reaction buffer of REDExtract-N-Amp PCR ReadyMix (Sigma) was used at concentration of 1× in 25 µl reaction mixtures per manufacturer instructions to obtain readily visible PCR products after 35–40 amplification cycles (30 s at 95 °C, 30 s at 50 °C and 1 min at 72 °C). The following primer sequences were used for identification of DNA: VSV-G 5'-TGAAGTGCCTTTTGTACTTAGCCTTTTTATTC-3' and 5'-ACCAGCGGAAATCACAAGTAGTGACC-3'; amp^R 5'-AATCAGTGAGGCACCTATCTCAGCG-3' and 5'-AAGCCATACCAAACGACGAGCG-3';

AluYd6 (human), 5' GAGATCGAGACCACGGTGAAA-3' and 5'-TTTGAGACGGAGTCTCGTT-3' as previously described (Walker et al., 2003); ACTB (human), 5'- CATGTACGTTGCTATCCAGGC-3', and 5'-ATTACCCACTCCCGACCCG (Primerbank ID 4501885a1). The amplification products were electrophoresed on 2% (wt/vol) agarose gel with subsequent ethidium bromide staining.

HIV passaging. Anonymous human PBMCs were provided by the UCLA Center for AIDS Research (CFAR) Virology Core Lab (peripheral blood). PBMCs were cultured in 5 μg ml^{-1} PHA (Sigma) in the presence of 5 ng ml^{-1} IL-2 (Peprotech) cells at 1 × 10^6 cells ml^{-1} and infected with 50 ng p24 of NL4-3 virus supernatant and incubated at 37 °C for 1 d. Infected cells were washed and and incubated again at 37 °C for 2 d. Uninfected cells were concurrently treated in an identical manner. Cell-free supernatant was collected and filtered through a 0.22 μm filter. Aliquots of cell-free supernatants were stored at –80 °C. All work was approved by the California Institute of Technology Institutional Biosafety Committee and Institutional Review Board exempt.

Statistical Analyses. GraphPad Prism 6.0 software was used for data analysis. Statistical significance was determined by unpaired, two-sided Student's *t*-tests for two groups or one-way ANOVA (with post-hoc Tukeys' multiple comparison test) for three or more groups.

FIGURE LEGENDS

Figure 1. Lentivector (LV) pseudotransduction delivers proteins and stimulates dendritic cells (DCs).

(A) Mouse bone marrow-derived DCs (BMDCs), human monocyte-derived DCs (moDCs), and 293T cells were incubated with tenofovir (TFV) 40 μM, efavirenz (EFV) 80 μM, or no drug (ND) 6 h prior to treatment with VSV-G-pseudotyped LV expressing GFP (LV-GFP(V)), and then analyzed 24 h later for GFP expression by flow cytometry.

(B) GFP mean fluorescent intensity (MFI) of DCs as treated in A.

(C) Mouse BMDCs were incubated with or without cycloheximide (CHX) for 1 h prior to treatment with LV-GFP(V) and GFP MFI measured by flow cytometry over 4 h. Results are presented relative to those of BMDCs receiving no LV with or without CHX.

(D) Western blot analysis of GFP of vector lysates from LV-GFP(V) and LV expressing ovalbumin (OVA) pseudotyped with VSV-G (LV-OVA(V)) and 40ng of purified GFP protein. Analysis of VSV-G was used as a loading control for the vectors.

(E,F) mouse BMDCs (E) and human moDCs (F) were treated as in A and analyzed for activation by measuring the MHC II molecule I-Ab and/or CD86 by flow cytometry. n.s.=not significant with $P > 0.05$; ***$P < 0.001$ (unpaired Student's t-test (B,D,F)). Data are representative of at least two independent experiments (A,B,D-F) or three independent experiments (C). Results are shown as mean ± s.e.m of technical replicates (B,C,E). See also Figure S1.

Figure 2. LV DNA, genome, and capsid are not required for DC maturation and $CD8^+$ T cell priming.

(A,B) Schematic diagram of VLPs and corresponding Western blot analysis for GFP, VSV-G, and p24 on LV and VLP lysates.

(C,D,E) Mouse BMDCs and human moDCs were treated with VSV-G or SVGmu-pseudotyped LVs and VLPs and then analyzed at 24 h for GFP, CD86, and I-Ab or HLA-DR expression by flow cytometry.

(F-I) Wild-type mice received homologous prime-boost vaccination of SVGmu-pseudotyped LV expressing OVA (LV-OVA) with or without RTI or SVGmu-pseudotyped VLP carrying OVA (VLP-OVA). (F) Flow cytometry analyzed the frequency of OVA-specific tetramer (H-2K^{b}-SIINFEKL)$^{+}$ CD8^{+} T cells from the blood at 7 and 10 d post-primary immunization. Numbers adjacent to outlined areas indicate percent of tetramer^{+} cells among the total CD8^{+} T cells. (G) Tetramer^{+} CD8^{+} T cells from the blood of immunized and unimmunized mice were measured by flow cytometry (black arrow, boost. (H) Flow cytometry analyzed CD62L and CD44 expression of tetramer^{+} CD8^{+} T cells from immunized mice compared or naïve CD8^{+} T cells from unimmunized mice at 41 d. (I) Seven wk post-boost, mice were injected with OVA-expressing and control tumor cells on opposing legs and tumor sizes measured.

(J,K) Wild-type mice were homologously prime-boosted with LV-OVA, VLP-OVA, or VLP without capsid carrying OVA (VLP-OVAΔgag). (J) Tetramer^{+} CD8^{+} T cells were measured from the blood. (K) Mice were injected with tumor cells as in I.

(L) Wild-type mice were injected with LV-OVA, LV encoding OVA carrying GFP (LV-GFP^{gene}-OVA^{protein}), or VLP-OVA. Tetramer^{+} CD8^{+} T cells were measured from the blood.

n.s.=not significant with $P > 0.05$; *$P < 0.05$; ***$P < 0.001$ (unpaired Student's t-test (C,D)). Data are representative of two independent experiments (B-E; mean ± s.e.m. of

technical replicates in C-E), one experiment (G-I; mean ± s.e.m. of *n* = 8 mice per group in E,G,H-J), or representative of two independent experiments (J-L; mean ± s.e.m. of *n* = 8 mice per group). See also Figure S2.

Figure 3. LV activation of DCs and subsequent CD8$^+$ T cell priming is dependent on STING, but not MyD88, TRIF, or IPS-1.

(A) BMDCs from mice deficient in MyD88, TRIF, and IPS-1 were treated with LV-GFP(V) or LV-GFP(S) and analyzed at 24 h for expression of CD86 and I-Ab by flow cytometry. (B-D) Mice deficient in MyD88, TRIF, IPS-1, or STING were immunized with LV-OVA. (B) Flow cytometry analyzed the frequency of OVA-specific tetramer$^+$ CD8$^+$ T cells from the blood at 10 d post-immunization. Numbers adjacent to outlined areas indicate percent of tetramer$^+$ cells among the total CD8$^+$ T cells. (C) Tetramer$^+$ CD8$^+$ T cells from the blood of immunized mutant and wild-type mice or unimmunized wild-type mice (*n* = 6 mice per group). Values between the groups of immunized mutant and wild-type mice at 10 d showed no statistical significance. (D,E) CD62L and CD44 expression of tetramer$^+$ CD8$^+$ T cells from immunized wild-type and mutant mice compared to naïve CD8$^+$ T cells from unimmunized wild-type mice at 10 d (*n* = 6 mice per group).

(F) Tetramer$^+$ CD8$^+$ T cells from the blood of immunized STING-deficient and wild-type mice (*n* = 5 mice per group).

(G) CD62L^{lo} and CD44$^+$ tetramer$^+$ CD8$^+$ T cells from STING-deficient and wild-type mice at 10 d (*n* = 5 mice per group).

Each symbol (C,E) represents the mean; error bars indicate s.e.m. Each symbol (E,G) represents an individual mouse; small horizontal lines indicate the mean. n.s., not significant, $P > 0.05$ (one way-ANOVA (A,C,E)); $*P < 0.05$ (unpaired Student's t-test (f)).

Data are from one experiment representative of three independent experiments (A; mean and s.e.m.), two independent experiment (B-E), or pooled from two experiments (F,G). See also Figures S1, S3, and S4.

Figure 4. Viral-like particles (VLPs) activate DCs and antigen-specific $CD8^+$ T cells via the STING pathway.

(A) BMDCs from STING-deficient and wild-type mice were treated with VLP carrying GFP pseudotyped with VSV-G (VLP-GFP(V)) or SVGmu (VLP-GFP(S)) and analyzed at 24 h for CD86 and I-Ab expression by flow cytometry.

(B) STING-deficient and wild-type BMDCs were treated with VLP-OVA pseudotyped with VSV-G (VLP-OVA(V)) or SVGmu (VLP-OVA(S)) and then cocultured with OT-1 $CD8^+$ T cells for 24 h. The $CD8^+$ T cells were analyzed for expression of activation markers CD69 and CD25 by flow cytometry.

(C-E) STING-deficient and wild-type mice were homologously prime-boosted with SVGmu-pseudotyped VLP-OVA. (C) Flow cytometry analyzed the frequency of OVA-specific $tetramer^+$ $CD8^+$ T cells from the blood at 7 d post-boost. Numbers adjacent to outlined areas indicate percent of $tetramer^+$ cells among the total $CD8^+$ T cells. (D) $Tetramer^+$ $CD8^+$ T cells from the blood of immunized STING-deficient and wild-type mice and unimmunized wild-type mice measured (black arrow, boost); (*n* = 8 mice per group). (E) $CD62L^{lo}$ and $CD44^+$ $tetramer^+$ $CD8^+$ T cells from STING-deficient and wild-type mice at 7 d post-boost (*n* = 8 mice per group).

Each symbol (D) represents the mean; error bars indicate s.e.m. Each symbol (E) represents an individual mouse; small horizontal lines indicate the mean. n.s., not significant, $P > 0.05$; $*P < 0.05$; $**P < 0.005$; $***P < 0.001$ (unpaired Student's t-test

(A,B,E)). Data are from one experiment representative of three independent experiments (A; error bars indicate s.e.m.), two independent experiments (B; error bars indicate s.e.m.), or pooled from two independent experiments (C-E).

Figure 5. Viral fusion is required for DC activation.

(A) Mouse BMDCs were incubated with chloroquine (CQ) at 25 μM, 75 μM, 100 μM (wedges) or no drug (ND) 1 h prior to treatment with LV or VLPs, and analyzed at 24 h for CD86 and I-Ab expression by flow cytometry.

(B) Fluorescence microscopy of mouse BMDCs treated with fusion-competent VLP-GFP(V) with or without CQ or fusion-defective VLP-GFP(V.FD). 400× magnification scale bar = 10 μm.

(C) Mouse BMDCs were infected with fusion-competent or fusion-defective LVs or VLPs carrying GFP and analyzed for CD86 and I-Ab expression.

(D,E) BMDCs from wild-type and STING-deficient mice were treated with naked (Lipo) or VSV-G enveloped multilamellar liposomes (Lipo(V)) carrying GFP and analyzed at 24 h for CD86 and I-Ab expression.

n.s., not significant, $P > 0.05$; ***$P < 0.001$ (unpaired Student's t-test (C,D,E)). Data are from one experiment representative of three independent experiments (A,C,D; error bars indicate s.e.m.) or two independent experiments (B,E; error bars indicate s.e.m.).

Figure 6. LV particles and VLPs contain human genomic DNA recognized by the host STING pathway.

(A) Amplicons of human β-actin (*ACTB*) and the ampicillin resistance gene (*amp*) detected in the LV and VLP preparations by PCR. The cell-free supernatant collected

from 293T cells transiently transfected with mock plasmid puc19 was used as a negative control.

(B) Amplicons of human Alu element (*Alu*) and VSV-G (*VSIVgp4)* were amplified from VLP preparations or genomic DNA (lane 1). VLP preparations or genomic DNA was treated with DNase I leading to DNA degradation (lane 2). If the DNase I was inactivated with EDTA before lysis, then DNA continued to be detected (lane 3). DNase I was inactivated with EDTA, and then VLP lysate added to show DNase I was effectively inactivated (lane 4).

(C) Amplicons of human DNA from 293T cellular genomic DNA treated in the same conditions as in B.

(D) PCR analysis for amplicons of human *ACTB* and *Alu* and plasmid from cell-free supernatant collected from 293T cells transiently transfected with the plasmid p.NL4-3 encoding infectious HIV-1 or 293T genomic DNA.

(E) NL4-3 HIV-1 was passaged in primary PBMCs and the cell-free supernatant was collected and analyzed for human *ACTB*. As a negative control, cell-free supernatant was collected from uninfected PBMCs.

(F) Amplicons of human *ACTB* and *Alu* were detected in cell-free supernatant containing NL4-3 HIV-1 passaged in primary PBMCs (lane 1). HIV-1 supernatant was treated with DNase I (lane 2), and then DNase I was inactivated by EDTA (lane 3) before lysis. DNase I was inactivated with EDTA and HIV lysate added to show DNase I was effectively inactivated (lane 4).

(G,H) BMDCs from STING-deficient or wild-type mice were treated with naked (Lipo) or VSV-G-enveloped multilamellar liposomes carrying plasmid DNA (Lipo-plasmid(V)),

genomic DNA extracted from 293T cells (Lipo-gDNA(V)), or nothing (Lipo(V)). Cells were analyzed 24 h post-treatment for CD86 and I-Ab expression by flow cytometry. n.s., not significant, $P > 0.05$; *$P < 0.05$; ***$P < 0.001$ (unpaired Student's t-test (G,H)). Data are from one experiment representative of three independent experiments (A-F) or two independent experiments (G,H; error bars indicate s.e.m.). See also Figure S5.

REFERENCES

ABE, A., MIYANOHARA, A. & FRIEDMANN, T. 1998. Enhanced gene transfer with fusogenic liposomes containing vesicular stomatitis virus G glycoprotein. *J Virol,* 72**,** 6159-63.

ARCE, F., ROWE, H. M., CHAIN, B., LOPES, L. & COLLINS, M. K. 2009. Lentiviral vectors transduce proliferating dendritic cell precursors leading to persistent antigen presentation and immunization. *Mol Ther,* 17**,** 1643-50.

BEIGNON, A. S., MCKENNA, K., SKOBERNE, M., MANCHES, O., DASILVA, I., KAVANAGH, D. G., LARSSON, M., GORELICK, R. J., LIFSON, J. D. & BHARDWAJ, N. 2005. Endocytosis of HIV-1 activates plasmacytoid dendritic cells via Toll-like receptor-viral RNA interactions. *J Clin Invest,* 115**,** 3265-75.

BERG, R. K., MELCHJORSEN, J., RINTAHAKA, J., DIGET, E., SOBY, S., HORAN, K. A., GORELICK, R. J., MATIKAINEN, S., LARSEN, C. S., OSTERGAARD, L., PALUDAN, S. R. & MOGENSEN, T. H. 2012. Genomic HIV RNA induces innate immune responses through RIG-I-dependent sensing of secondary-structured RNA. *PLoS One,* 7**,** e29291.

BERNIER, R. & TREMBLAY, M. 1995. Homologous interference resulting from the presence of defective particles of human immunodeficiency virus type 1. *J Virol,* 69**,** 291-300.

BONIFAZ, L., BONNYAY, D., MAHNKE, K., RIVERA, M., NUSSENZWEIG, M. C. & STEINMAN, R. M. 2002. Efficient targeting of protein antigen to the dendritic cell receptor DEC-205 in the steady state leads to antigen presentation on major histocompatibility complex class I products and peripheral CD8+ T cell tolerance. *J Exp Med,* 196**,** 1627-38.

BRECKPOT, K., DULLAERS, M., BONEHILL, A., VAN MEIRVENNE, S., HEIRMAN, C., DE GREEF, C., VAN DER BRUGGEN, P. & THIELEMANS, K. 2003. Lentivirally transduced dendritic cells as a tool for cancer immunotherapy. *J Gene Med,* 5**,** 654-67.

BRECKPOT, K., EMEAGI, P., DULLAERS, M., MICHIELS, A., HEIRMAN, C. & THIELEMANS, K. 2007. Activation of immature monocyte-derived dendritic cells after transduction with high doses of lentiviral vectors. *Hum Gene Ther,* 18**,** 536-46.

BRECKPOT, K., ESCORS, D., ARCE, F., LOPES, L., KARWACZ, K., VAN LINT, S., KEYAERTS, M. & COLLINS, M. 2010. HIV-1 lentiviral vector immunogenicity is mediated by Toll-like receptor 3 (TLR3) and TLR7. *J Virol,* 84**,** 5627-36.

CHINNASAMY, N., CHINNASAMY, D., TOSO, J. F., LAPOINTE, R., CANDOTTI, F., MORGAN, R. A. & HWU, P. 2000. Efficient gene transfer to human peripheral blood monocyte-derived dendritic cells using human immunodeficiency virus type 1-based lentiviral vectors. *Hum Gene Ther,* 11**,** 1901-9.

COWAN, S., HATZIIOANNOU, T., CUNNINGHAM, T., MUESING, M. A., GOTTLINGER, H. G. & BIENIASZ, P. D. 2002. Cellular inhibitors with Fv1-like activity restrict human and simian immunodeficiency virus tropism. *Proc Natl Acad Sci U S A,* 99**,** 11914-9.

DAI, B., YANG, L., YANG, H., HU, B., BALTIMORE, D. & WANG, P. 2009. HIV-1 Gag-specific immunity induced by a lentivector-based vaccine directed to dendritic cells. *Proc Natl Acad Sci U S A,* 106**,** 20382-7.

DILLE, B. J. & JOHNSON, T. C. 1982. Inhibition of vesicular stomatitis virus glycoprotein expression by chloroquine. *J Gen Virol,* 62 (Pt 1)**,** 91-103.

DOITSH, G., GALLOWAY, N. L., GENG, X., YANG, Z., MONROE, K. M., ZEPEDA, O., HUNT, P. W., HATANO, H., SOWINSKI, S., MUNOZ-ARIAS, I. & GREENE, W. C. 2014. Cell death by pyroptosis drives CD4 T-cell depletion in HIV-1 infection. *Nature,* 505**,** 509-14.

DULLAERS, M., VAN MEIRVENNE, S., HEIRMAN, C., STRAETMAN, L., BONEHILL, A., AERTS, J. L., THIELEMANS, K. & BRECKPOT, K. 2006. Induction of effective therapeutic antitumor immunity by direct in vivo administration of lentiviral vectors. *Gene Ther,* 13**,** 630-40.

DYALL, J., LATOUCHE, J. B., SCHNELL, S. & SADELAIN, M. 2001. Lentivirus-transduced human monocyte-derived dendritic cells efficiently stimulate antigen-specific cytotoxic T lymphocytes. *Blood,* 97**,** 114-21.

ELOUAHABI, A. & RUYSSCHAERT, J. M. 2005. Formation and intracellular trafficking of lipoplexes and polyplexes. *Mol Ther,* 11**,** 336-47.

ESSLINGER, C., CHAPATTE, L., FINKE, D., MICONNET, I., GUILLAUME, P., LEVY, F. & MACDONALD, H. R. 2003. In vivo administration of a lentiviral vaccine targets DCs and induces efficient CD8(+) T cell responses. *J Clin Invest,* 111**,** 1673-81.

FLORKIEWICZ, R. Z. & ROSE, J. K. 1984. A cell line expressing vesicular stomatitis virus glycoprotein fuses at low pH. *Science,* 225**,** 721-3.

GALLA, M., WILL, E., KRAUNUS, J., CHEN, L. & BAUM, C. 2004. Retroviral pseudotransduction for targeted cell manipulation. *Mol Cell,* 16**,** 309-15.

GAO, D., WU, J., WU, Y. T., DU, F., AROH, C., YAN, N., SUN, L. & CHEN, Z. J. 2013. Cyclic GMP-AMP synthase is an innate immune sensor of HIV and other retroviruses. *Science,* 341**,** 903-6.

GRANELLI-PIPERNO, A., ZHONG, L., HASLETT, P., JACOBSON, J. & STEINMAN, R. M. 2000. Dendritic cells, infected with vesicular stomatitis virus-pseudotyped HIV-1, present viral antigens to CD4+ and CD8+ T cells from HIV-1-infected individuals. *J Immunol,* 165**,** 6620-6.

HAAS, D. L., CASE, S. S., CROOKS, G. M. & KOHN, D. B. 2000. Critical factors influencing stable transduction of human CD34(+) cells with HIV-1-derived lentiviral vectors. *Mol Ther,* 2**,** 71-80.

HE, Y. & FALO, L. D. 2007. Lentivirus as a potent and mechanistically distinct vector for genetic immunization. *Current Opinion in Molecular Therapeutics,* 9**,** 439-446.

HE, Y., ZHANG, J., MI, Z., ROBBINS, P. & FALO, L. D., JR. 2005. Immunization with lentiviral vector-transduced dendritic cells induces strong and long-lasting T cell responses and therapeutic immunity. *J Immunol,* 174**,** 3808-17.

HOLM, C. K., JENSEN, S. B., JAKOBSEN, M. R., CHESHENKO, N., HORAN, K. A., MOELLER, H. B., GONZALEZ-DOSAL, R., RASMUSSEN, S. B., CHRISTENSEN, M. H., YAROVINSKY, T. O., RIXON, F. J., HEROLD, B. C., FITZGERALD, K. A. & PALUDAN, S. R. 2012. Virus-cell fusion as a trigger of innate immunity dependent on the adaptor STING. *Nat Immunol,* 13**,** 737-43.

HU, B., TAI, A. & WANG, P. 2011. Immunization delivered by lentiviral vectors for cancer and infectious diseases. *Immunol Rev,* 239**,** 45-61.

ISHIKAWA, H., MA, Z. & BARBER, G. N. 2009. STING regulates intracellular DNA-mediated, type I interferon-dependent innate immunity. *Nature,* 461**,** 788-92.

JAKOBSEN, M. R., BAK, R. O., ANDERSEN, A., BERG, R. K., JENSEN, S. B., TENGCHUAN, J., LAUSTSEN, A., HANSEN, K., OSTERGAARD, L.,

FITZGERALD, K. A., XIAO, T. S., MIKKELSEN, J. G., MOGENSEN, T. H. & PALUDAN, S. R. 2013. IFI16 senses DNA forms of the lentiviral replication cycle and controls HIV-1 replication. *Proc Natl Acad Sci U S A,* 110**,** E4571-80.

KNUDSEN, K. B., NORTHEVED, H., KUMAR, P. E., PERMIN, A., GJETTING, T., ANDRESEN, T. L., LARSEN, S., WEGENER, K. M., LYKKESFELDT, J., JANTZEN, K., LOFT, S., MOLLER, P. & ROURSGAARD, M. 2015. In vivo toxicity of cationic micelles and liposomes. *Nanomedicine,* 11**,** 467-77.

LIU, Y., FANG, J., JOO, K. I., WONG, M. K. & WANG, P. 2014. Codelivery of chemotherapeutics via crosslinked multilamellar liposomal vesicles to overcome multidrug resistance in tumor. *PLoS One,* 9**,** e110611.

MANEL, N., HOGSTAD, B., WANG, Y., LEVY, D. E., UNUTMAZ, D. & LITTMAN, D. R. 2010. A cryptic sensor for HIV-1 activates antiviral innate immunity in dendritic cells. *Nature,* 467**,** 214-7.

MANGEOT, P. E., DOLLET, S., GIRARD, M., CIANCIA, C., JOLY, S., PESCHANSKI, M. & LOTTEAU, V. 2011. Protein transfer into human cells by VSV-G-induced nanovesicles. *Mol Ther,* 19**,** 1656-66.

METHAROM, P., ELLEM, K. A., SCHMIDT, C. & WEI, M. Q. 2001. Lentiviral vector-mediated tyrosinase-related protein 2 gene transfer to dendritic cells for the therapy of melanoma. *Hum Gene Ther,* 12**,** 2203-13.

MOORE, P. L., CROOKS, E. T., PORTER, L., ZHU, P., CAYANAN, C. S., GRISE, H., CORCORAN, P., ZWICK, M. B., FRANTI, M., MORRIS, L., ROUX, K. H., BURTON, D. R. & BINLEY, J. M. 2006. Nature of nonfunctional envelope proteins on the surface of human immunodeficiency virus type 1. *J Virol,* 80**,** 2515-28.

NASH, K. L. & LEVER, A. M. 2004. Green fluorescent protein: green cells do not always indicate gene expression. *Gene Ther,* 11**,** 882-3.

ODEGARD, J. M., KELLEY-CLARKE, B., TAREEN, S. U., CAMPBELL, D. J., FLYNN, P. A., NICOLAI, C. J., SLOUGH, M. M., VIN, C. D., MCGOWAN, P. J., NELSON, L. T., TER MEULEN, J., DUBENSKY, T. W., JR. & ROBBINS, S. H. 2015. Virological and preclinical characterization of a dendritic cell targeting, integration-deficient lentiviral vector for cancer immunotherapy. *J Immunother,* 38**,** 41-53.

PICHLMAIR, A., DIEBOLD, S. S., GSCHMEISSNER, S., TAKEUCHI, Y., IKEDA, Y., COLLINS, M. K. & REIS E SOUSA, C. 2007. Tubulovesicular structures within vesicular stomatitis virus G protein-pseudotyped lentiviral vector preparations carry DNA and stimulate antiviral responses via Toll-like receptor 9. *J Virol,* 81**,** 539-47.

ROUAS, R., UCH, R., CLEUTER, Y., JORDIER, F., BAGNIS, C., MANNONI, P., LEWALLE, P., MARTIAT, P. & VAN DEN BROEKE, A. 2002. Lentiviral-mediated gene delivery in human monocyte-derived dendritic cells: optimized design and procedures for highly efficient transduction compatible with clinical constraints. *Cancer Gene Ther,* 9**,** 715-24.

SCHROERS, R., SINHA, I., SEGALL, H., SCHMIDT-WOLF, I. G., ROONEY, C. M., BRENNER, M. K., SUTTON, R. E. & CHEN, S. Y. 2000. Transduction of human PBMC-derived dendritic cells and macrophages by an HIV-1-based lentiviral vector system. *Mol Ther,* 1**,** 171-9.

SHA, W. C., LIOU, H. C., TUOMANEN, E. I. & BALTIMORE, D. 1995. Targeted disruption of the p50 subunit of NF-kappa B leads to multifocal defects in immune responses. *Cell,* 80**,** 321-30.

SHEN, Y. J., LE BERT, N., KOO, C.X., HO, S.S., ISHII, K.J., RAULET, D.H., GASSER, S. 2014. Tumor cells express genome-derived DNA in the cytosol. *Cancer Res* 74**,** 3168.

SKELTON, D., SATAKE, N. & KOHN, D. B. 2001. The enhanced green fluorescent protein (eGFP) is minimally immunogenic in C57BL/6 mice. *Gene Ther,* 8**,** 1813-4.

SMIT, J. M., BITTMAN, R. & WILSCHUT, J. 1999. Low-pH-dependent fusion of Sindbis virus with receptor-free cholesterol- and sphingolipid-containing liposomes. *J Virol,* 73**,** 8476-84.

SOMAIAH, N., BLOCK, M.S., KIM, J.W., SHAPIRO, G., HWU, P., EDER, J.P., JONES, R.L., GNJATIC, S., LU, H., HSU. F.J., POLLACK, S. 2015. Phase I, first-in-human trial of LV305 in patients with advanced or metastatic cancer expressing NY-ESO-1. *Journal of Clinical Oncology,* 33**,** 3021.

SUN, L., WU, J., DU, F., CHEN, X. & CHEN, Z. J. 2013. Cyclic GMP-AMP synthase is a cytosolic DNA sensor that activates the type I interferon pathway. *Science,* 339**,** 786-91.

WALKER, J. A., KILROY, G. E., XING, J., SHEWALE, J., SINHA, S. K. & BATZER, M. A. 2003. Human DNA quantitation using Alu element-based polymerase chain reaction. *Anal Biochem,* 315**,** 122-8.

YANG, L., YANG, H., RIDEOUT, K., CHO, T., JOO, K. I., ZIEGLER, L., ELLIOT, A., WALLS, A., YU, D., BALTIMORE, D. & WANG, P. 2008. Engineered lentivector targeting of dendritic cells for in vivo immunization. *Nat Biotechnol,* 26**,** 326-34.

ZHANG, L. & GHOSH, H. P. 1994. Characterization of the putative fusogenic domain in vesicular stomatitis virus glycoprotein G. *J Virol,* 68**,** 2186-93.

ZHU, W., LI, J., TANG, L., WANG, H., LI, J., FU, J. & LIANG, G. 2011. Glycoprotein is enough for sindbis virus-derived DNA vector to express heterogenous genes. *Virol J,* 8**,** 344.

SUPPLEMENTAL FIGURE LEGENDS

Figure S1. LVs pseudotransduce and activate mouse BMDCs, related to Figures 1 and 3. Mouse BMDCs were treated with LV-GFP(V), LV-GFP(S), LPS, or no vector (NV) and analyzed for expression of GFP, CD86, and I-Ab by flow cytometry.

(A) Numbers adjacent to outlined areas are the GFP MFI values of the CD11c+CD11b+ cells immediate post-LV treatment.

(B) Numbers adjacent to outlined areas are the percent activated CD11c+CD11b+ cells.

(C, D) Time course of the expression of GFP, CD86+ and I-Ab+ BMDCs over 48 h. Each symbol represents the mean; error bars indicate s.e.m. Data are from (A) one experiment representative of five independent experiments or from two independent experiments (B-D). See also Figures 1 and 2.

Figure S2. LVs and VLPs carry heterologous proteins, related to Figure 2.

(A) Western blot analysis of GFP and VSV-G from the viral lysates of LV-GFP(V) and LV expressing ovalbumin (OVA) pseudotyped with SVGmu (LV-OVA(S)).

(B) Western blot analysis for GFP or OVA from the viral lysate of VSVG or SVGmu-pseudotyped VLPs carrying GFP or OVA.

(C) Western blot analysis of OVA in the lysate of SVGmu-pseudotyped VLP carrying OVA. VLP carrying OVA was not treated with proteinase K (PK) or PMSF (lane 1). VLP was pre-treated with PK, and then the PK was inactivated with PMSF before lysis (lane 2). To verify PK degradation was effective, PK was not inactivated before VLP lysis (lane 3). See also Figure 1.

Figure S3. MyD88-/-/TRIFLps2/Lps2 or MyD88-/-/IPS-1-/- BMDCs are fully activated by LVs, related to Figure 3.

(A,B) BMDCs from mice doubly deficient in MyD88 and TRIF (A) or MyD88 and IPS-1 (B) were treated with LV-GFP(V) or LV-GFP(S) and analyzed 24 h post-treatment for the percentage of

CD86 and I-Ab-positive cells by flow cytometry. n.s., not significant, P > 0.05 (unpaired Student's t-test). Data from three independent experiments (mean and s.e.m.). See also Figure 3.

Figure S4. Normal T cell subsets in STING-deficient mice under non-stimulatory conditions, related to Figure 3.

(A, B) Splenocytes from STING-deficient or wild-type mice were analyzed by flow cytometry using anti-CD4 and anti-CD8 under non-stimulated conditions.

(C) Wild-type and STING-deficient splenocytes were treated with PMA (50ng/ml) and ionomycin (500ng/ml) and cells were analyzed at 24 h, 48 h, and 72 h post-treatment. Surface expression of CD69 and CD25 of the gated CD8+ T cells was measured by flow cytometry. n.s., not significant, P > 0.05 (unpaired Student's t-test). Data from two independent experiment (mean and s.e.m) (A-C). See also Figure 3.

Figure S5. LV particles and VLPs contain human genomic DNA, related to Figure 6.

(A,B) Amplicons of VSV-G (VSIVgp4) and human Alu repeat element (Alu) in the LV and VLP preparations by PCR. See also Figure 5.

FIGURES

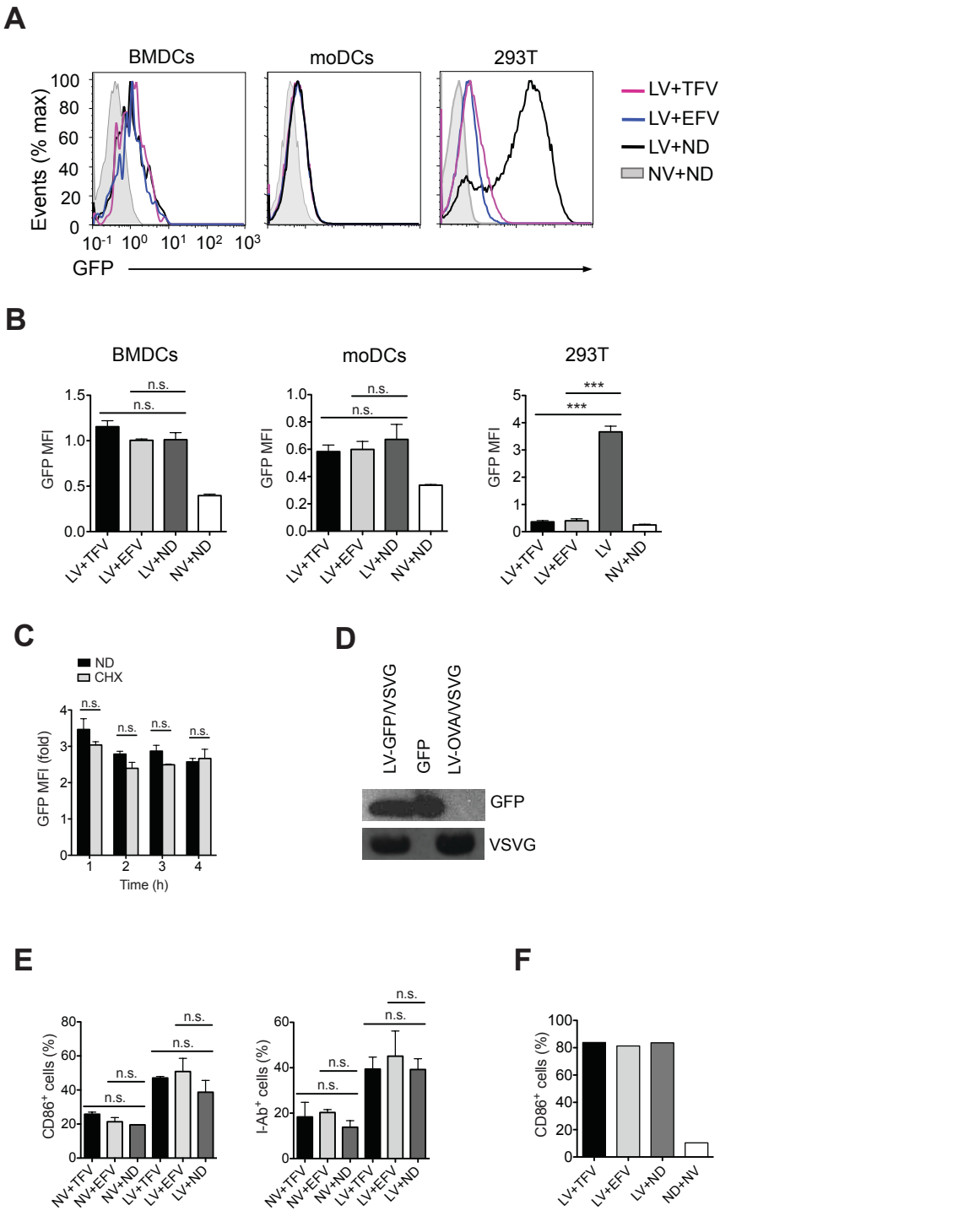

Figure 1. Lentivector (LV) pseudotransduction delivers proteins and stimulates dendritic cells (DCs).

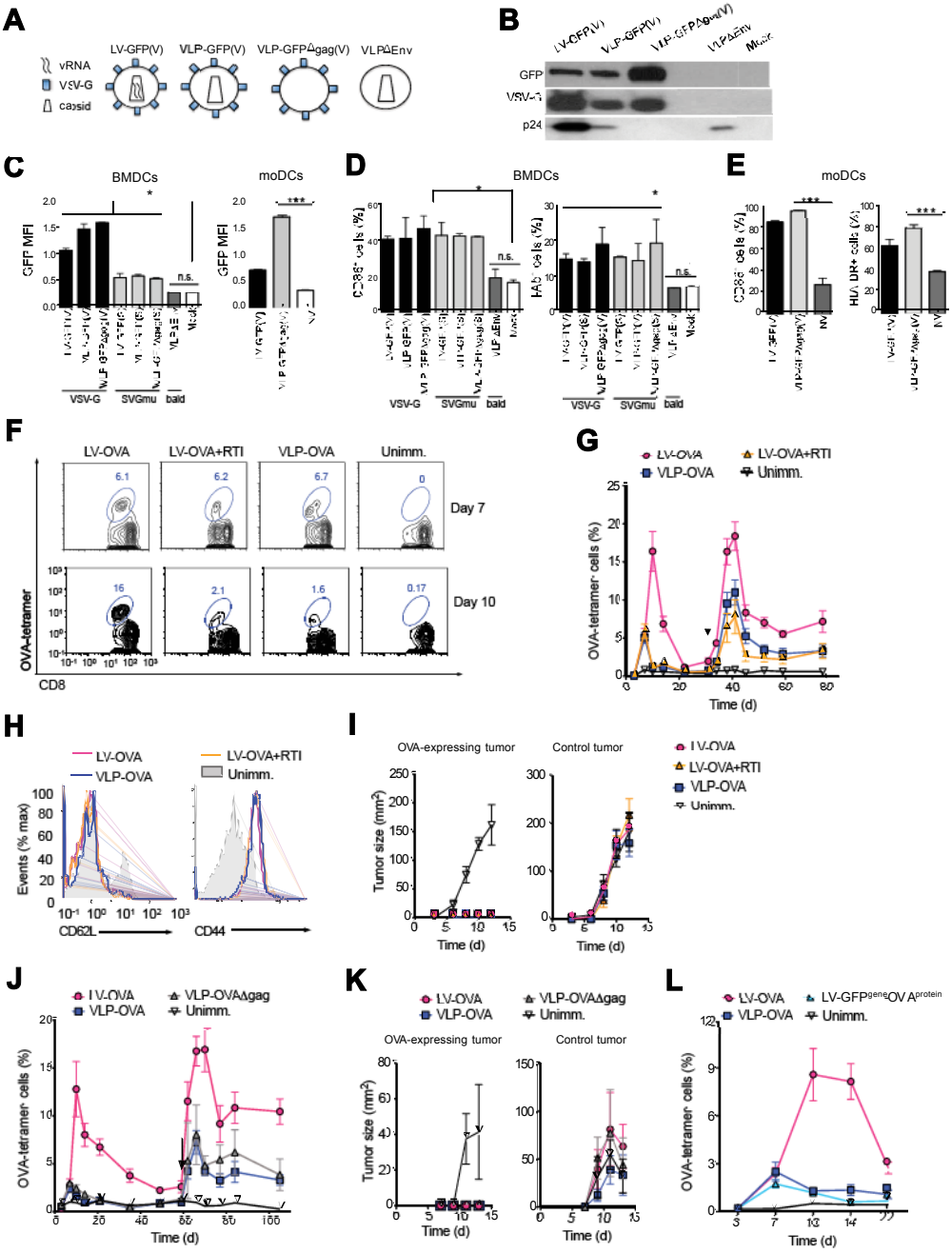

Figure 2. LV DNA, genome, and capsid are not required for DC maturation and CD8$^+$ T cell priming.

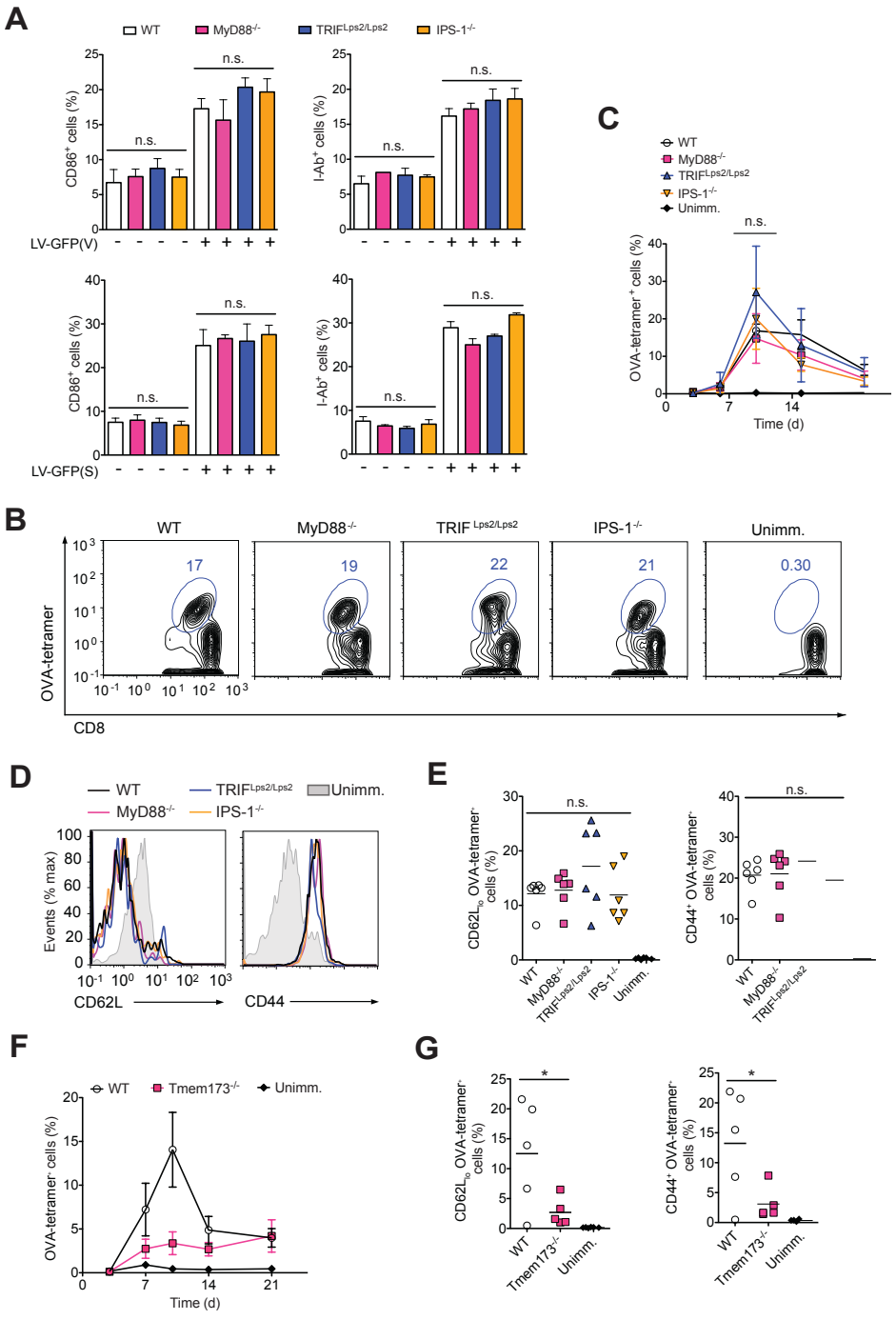

Figure 3. LV activation of DCs and subsequent CD8$^+$ T cell priming is dependent on STING, but not MyD88, TRIF, or IPS-1.

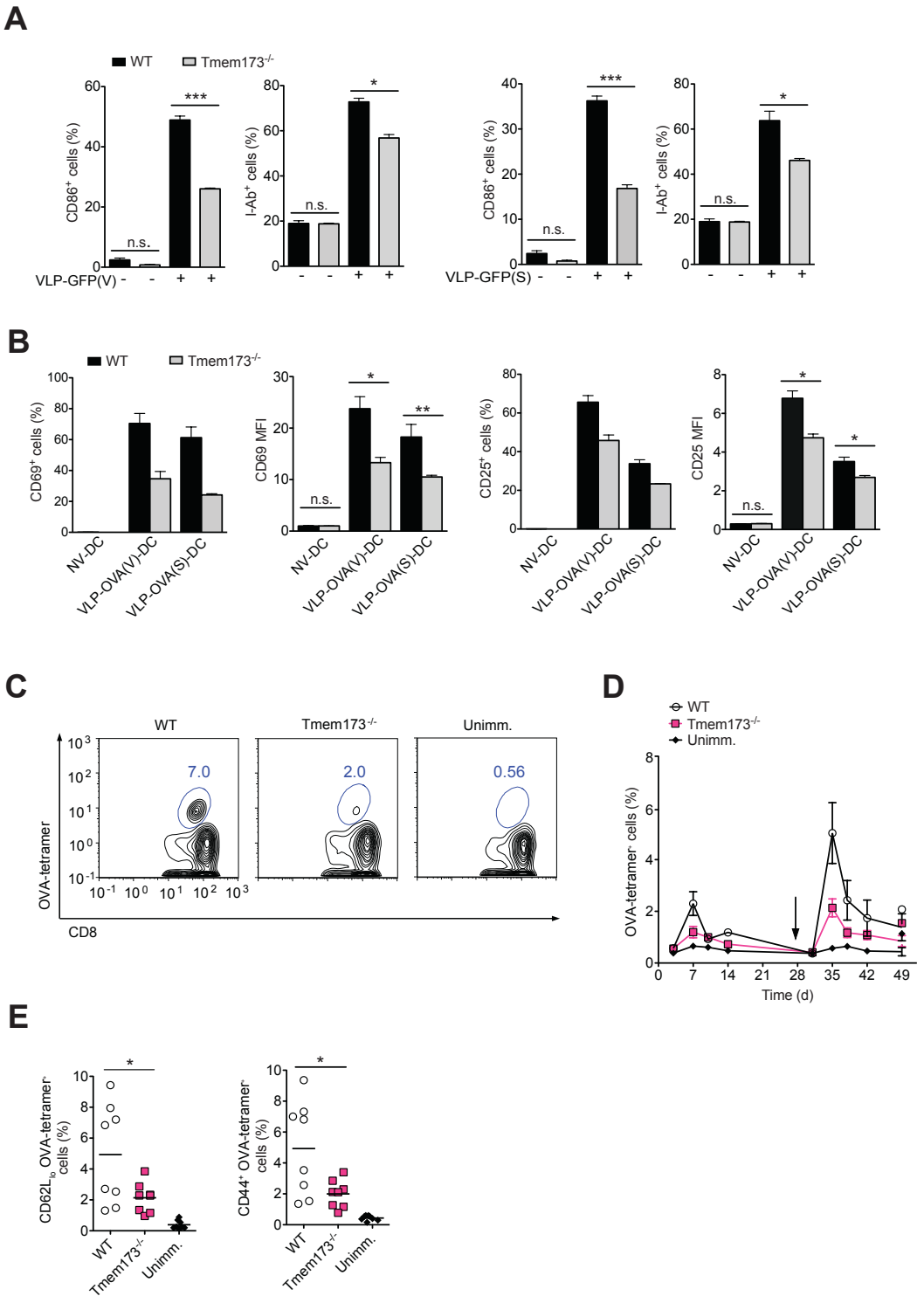

Figure 4. Viral-like particles (VLPs) activate DCs and antigen-specific CD8$^+$ T cells via the STING pathway.

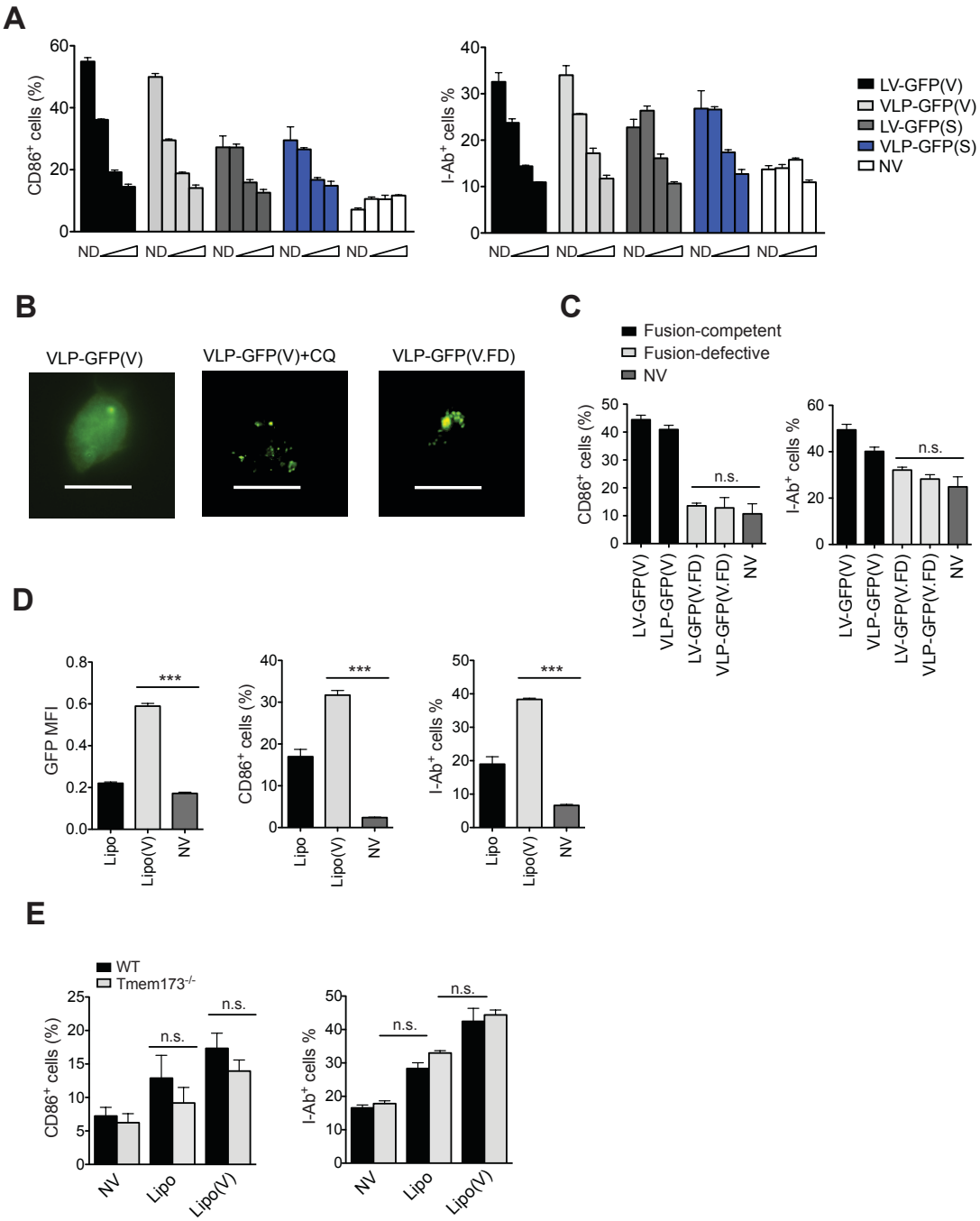

Figure 5. Viral fusion is required for DC activation.

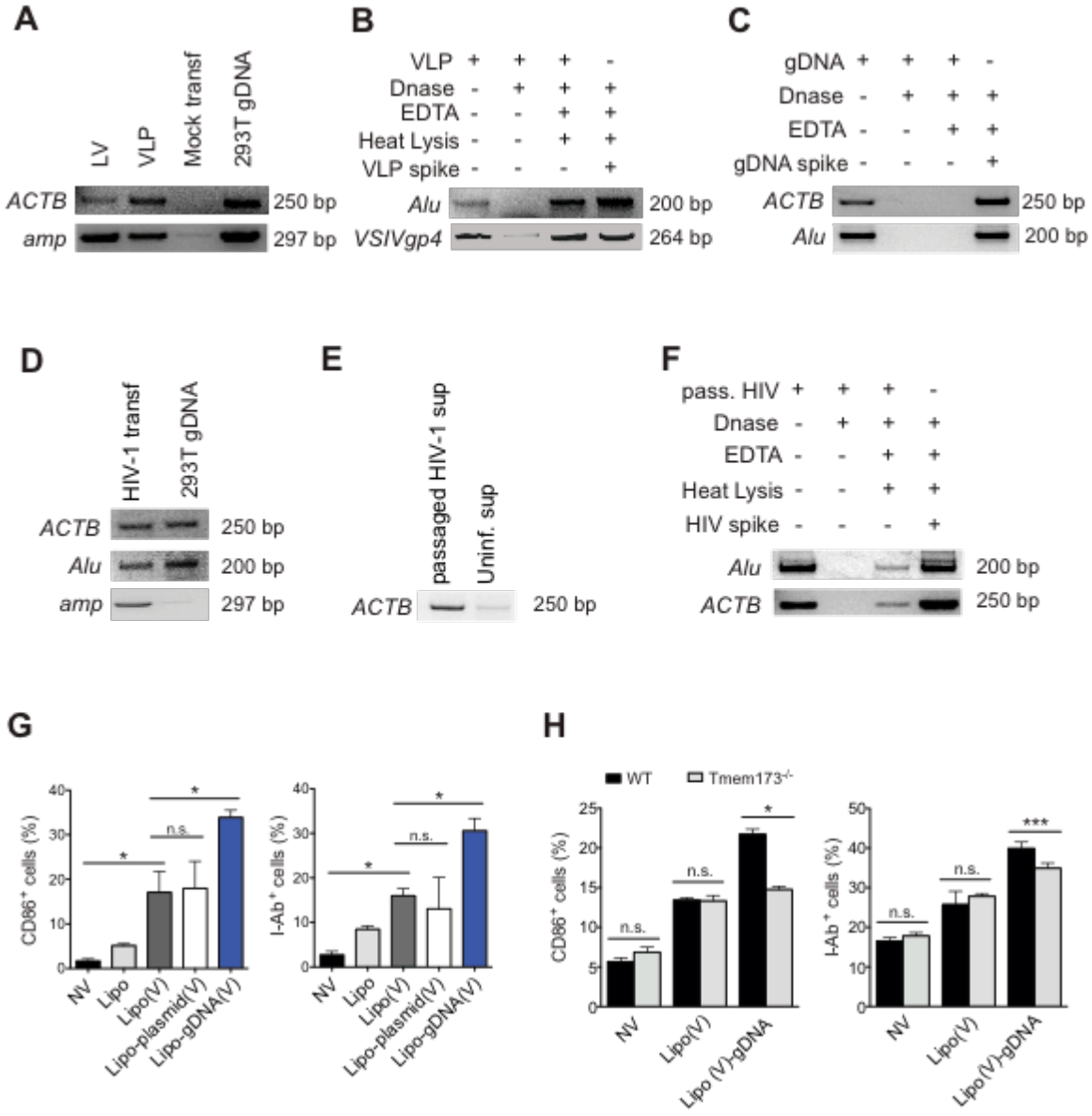

Figure 6. LV particles and VLPs contain human genomic DNA recognized by the host STING pathway.

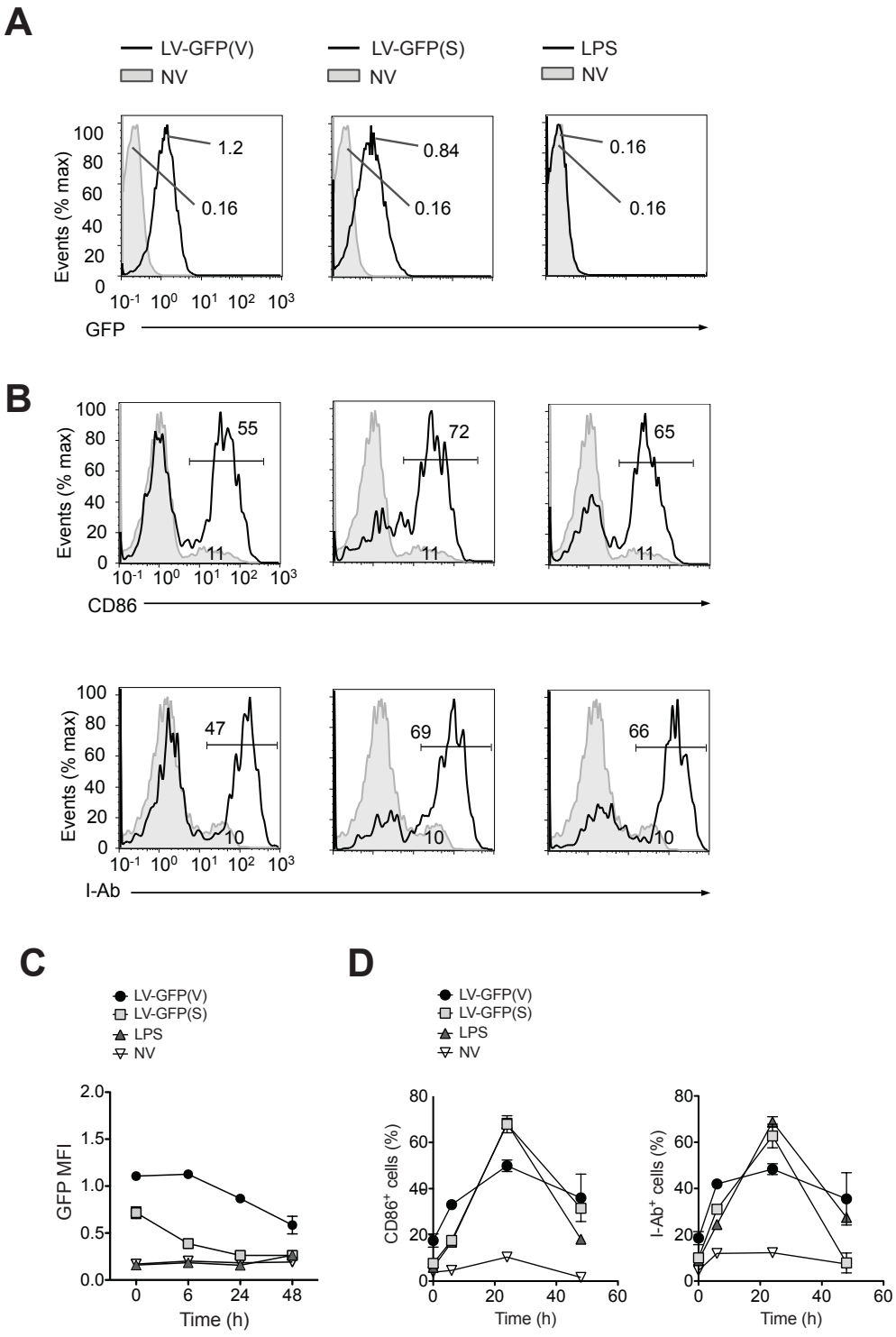

Figure S1. LVs pseudotransduce and activate mouse BMDCs, related to Figures 1 and 3.

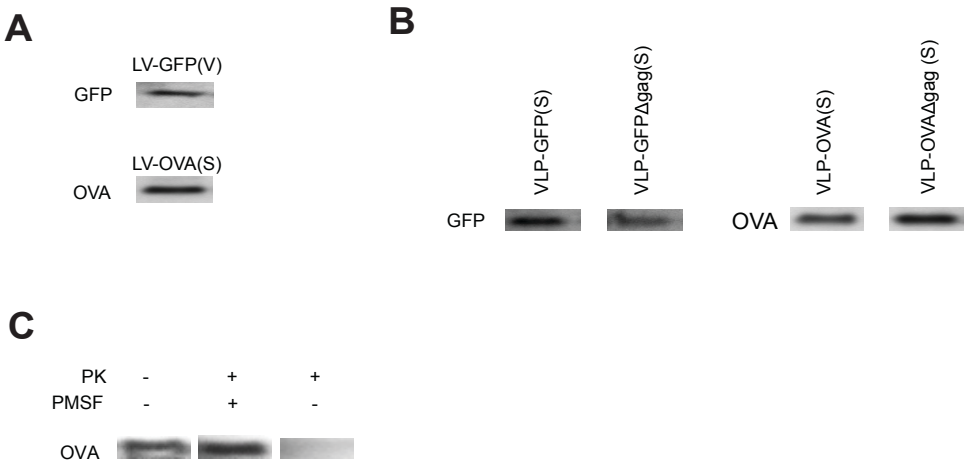

Figure S2. LVs and VLPs carry heterologous proteins, related to Figure 2.

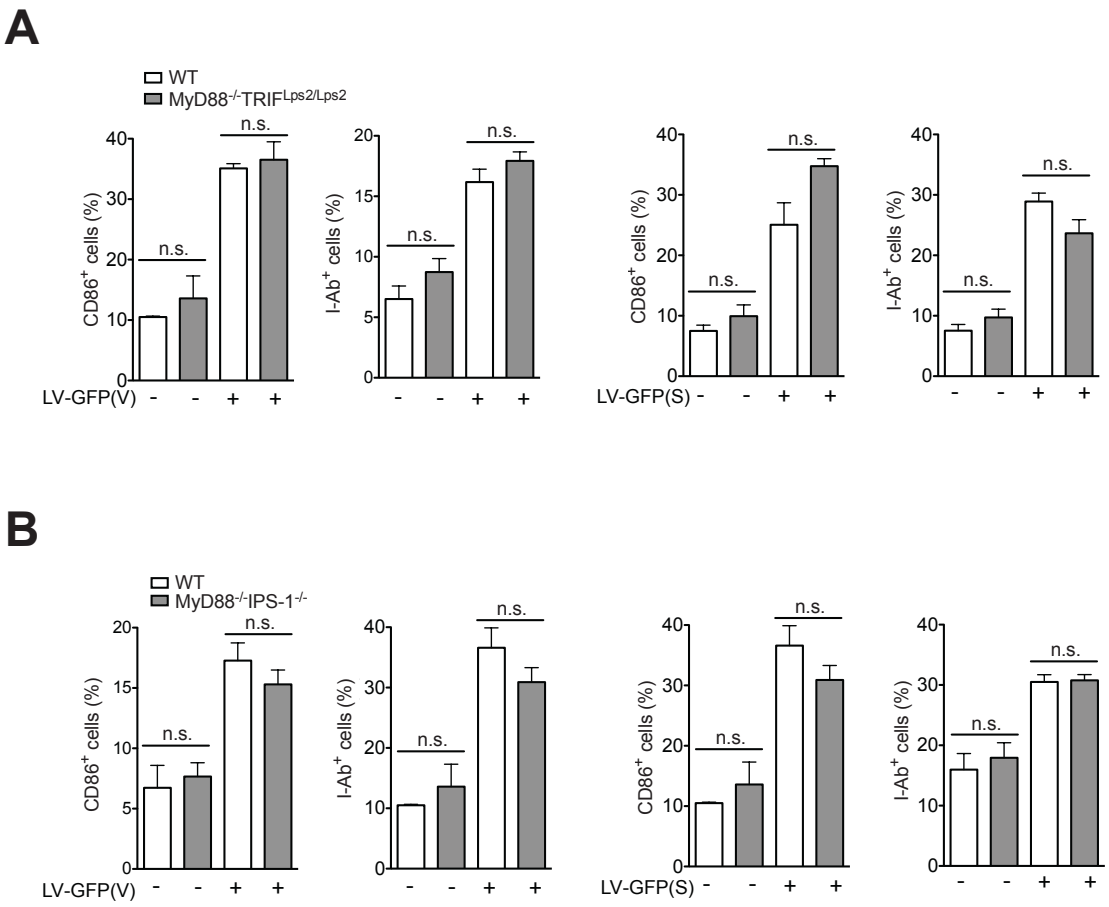

Figure S3. MyD88-/-/TRIFLps2/Lps2 or MyD88-/-/IPS-1-/- BMDCs are fully activated by LVs, related to Figure 3.

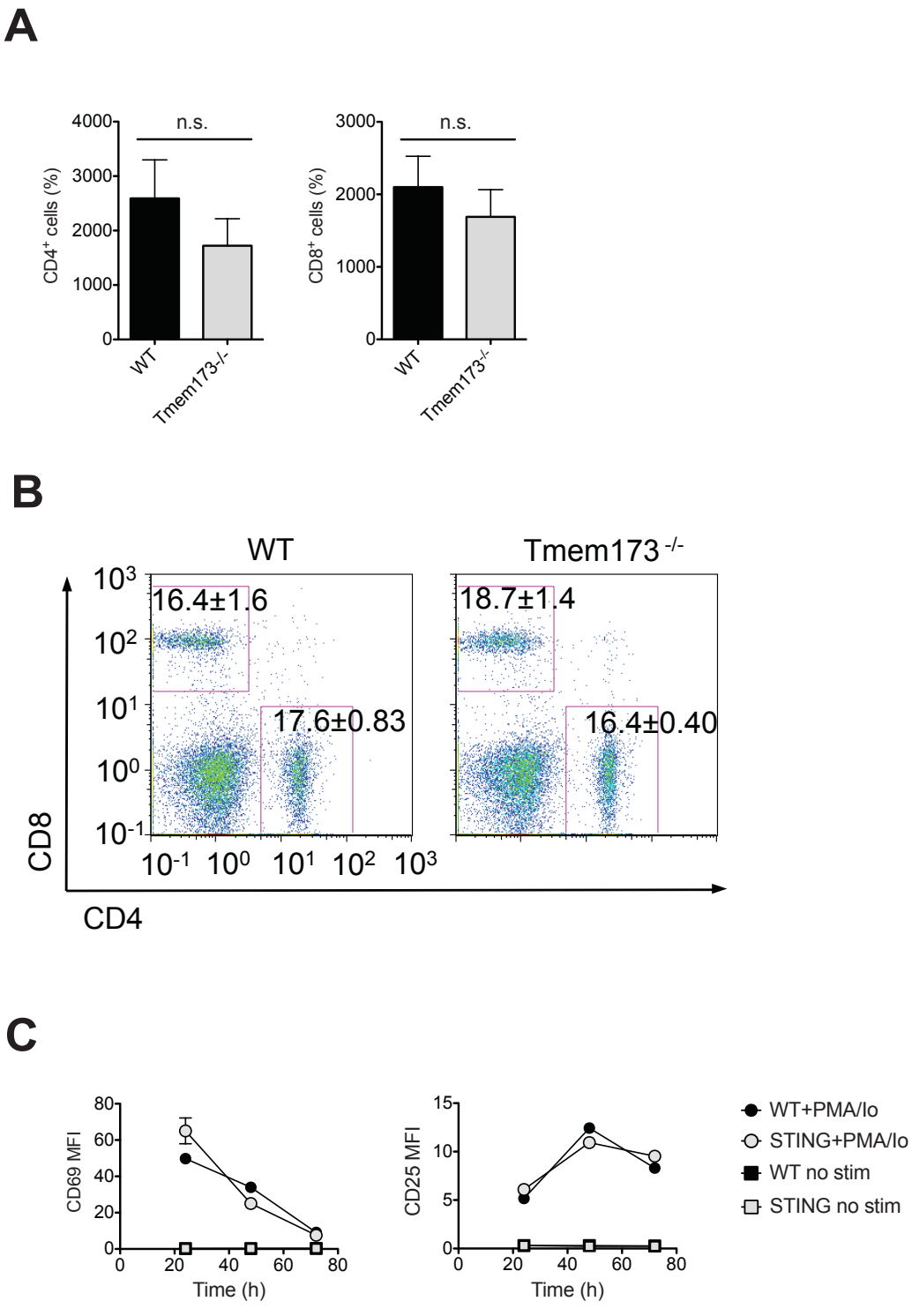

Figure S4. Normal T cell subsets in STING-deficient mice under non-stimulatory conditions, related to Figure 3.

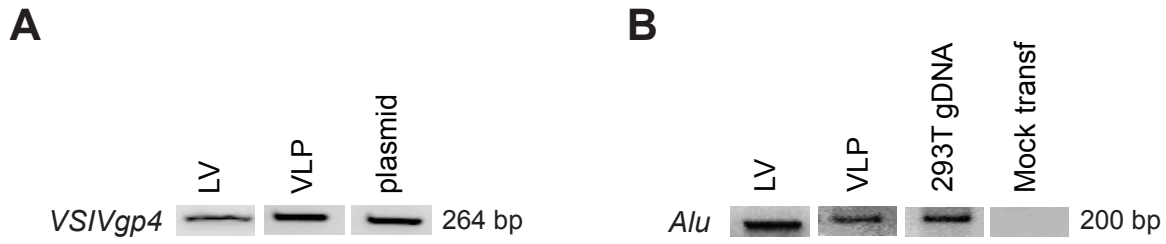

Figure S5. LV particles and VLPs contain human genomic DNA, related to Figure 6.